

Spatiotemporal Variation of Demographic Parameters and Seasonal Habitat Fidelity by Moose in Idaho

A Thesis

Presented in Partial Fulfillment of the Requirements for the

Degree of Master of Science

with a

Major in Natural Resources

in the

College of Graduate Studies

University of Idaho

by

Eric T. Van Beek

Approved by:

Major Professor: Janet L. Rachlow, Ph.D.

Committee Members: Jon S. Horne, Ph.D.; Ryan A. Long, Ph.D.

Department Administrator: Janet L. Rachlow, Ph.D.

December 2023

Abstract

Hunter harvest and aerial survey data suggest that some moose populations in Idaho have been declining since the mid-1990s. However, longitudinal demographic data spanning the range of moose in Idaho are lacking, making it difficult to explain observed trends. We initiated a multi-year project in January 2020 to better understand population dynamics and habitat use by moose in Idaho. During January-March 2020 and 2021, we fitted 148 adult females and 17 9-month-old calves with GPS collars in 5 regions throughout Idaho, USA. We monitored collared moose to document survival and to facilitate investigation of mortalities. To document parturition rates and summer calf survival, we conducted ground observations of parturient collared females during May-August 2020-2022. We also used resource selection functions (RSF) to model and predict resource use by moose during a critical timeframe in the life cycle of an important parasite of moose, the winter tick (*Dermacentor albipictus*). Results from region specific RSFs were used to predict the relative probability of tick occurrence on the landscape which we interpreted as the “the tick risk landscape”. We then modeled the relationship between the tick risk landscape and relative tick burden on moose assessed at the time of capture. Our results indicated that moose populations were relatively stable during the study period. Furthermore, we found that spatiotemporal variation in population growth was almost completely correlated with spatiotemporal variation in adult female survival. This finding suggests that adult female survival is primarily responsible for observed population growth and should be a target for management action. We also found that as moose spent more time within the tick risk landscape, they acquired more ticks. The tick risk landscape can be used in future research to estimate tick load on moose and provide spatial boundaries for tick reduction efforts.

Acknowledgments

This project has been a culmination of the knowledge, effort, and insight from countless individuals. First and foremost, I would like to thank my major advisor Dr. Janet Rachlow. Your support, guidance and encouragement throughout every stage of this project has been instrumental in completion of this thesis and my development as a student and wildlife professional.

Thank you to my committee members Dr. Ryan Long and Dr. Jon Horne for your insight towards project design and analyses. A special thank you to Jon for the long days (and nights) spent coding and working through analyses. I can't begin to explain how much I learned throughout the process and would be lying if I said it wasn't fun (even if it was type 2 fun). Thank you to my lab mate Logan Weyand for everything from project planning to January moose necropsies. Your passion for wildlife and immense knowledge of all things wildlife health has been integral to the outcome of this project.

This project would not have been possible without the assistance from the Idaho Department of Fish and Game. Thank you to Mark Hurley, Shane Roberts, and Hollie Miyasaki for help designing research goals, developing questions, coordinating field gear and trucks, and ultimately being an invaluable resource for the broader scope of this project. Thank you to Stacey Dauwalter, Nicole Walrath, Tricia Hebdon, and others at the Wildlife Health Lab for everything wildlife health related. From coordinating necropsies to data organization, and inundating your freezers with moose parts, you all greatly simplified things on our end. I am very grateful to regional staff that assisted with capture, coordinating field gear, housing, necropsies and anything else that came up: Micah Ellstrom, Barb Moore, Laura Wolf, Clay Hickey, Jana Livingston, Mike McDonald, Jake Powell, Sierra Robotcek, Zach Lockyer, Eric Freeman, Curtis Hendricks, Morgan Pfander, and Iver Hull. Having you

all as resources throughout our study regions put my mind at ease while out checking on moose and streamlined the entire project. Thank you to Michelle Kemner for putting GPS collars and kits together and being an exceptional resource for any capture or collar questions. Thank you to Kayte Groth for dealing with all our vehicle needs and letting us max out your P-card multiple times for vehicle repairs. To the countless other IDFG technicians, conservation officers, and biologists that assisted with various aspects of this project and took on responsibilities well outside of your typical job duties, thank you all for your time and effort, it does not go unnoticed and definitely does not go underappreciated.

Thank you to Tony Herbie and Kerry Croft with 307 aviation for the safe flying and putting us within arm's reach of moose, Paul Atwood for coordinating capture and putting darts where they need to be, and Dan Melody and Owyhee air for finding moose calves much more efficiently than we could have from the ground.

Looking for baby moose calves seems like a laid-back gig, but as all the technicians from this project know, it's easier said than done. Brian Sewell, Luke Benzinger, John Nally, Kiwi Sheldon, Kevin Gerena, Ryan Harris, Miranda Reinson, and Lucas Begeman, thank you for all the miles hiked, hours of windshield time, sunburns, tick bites, and climbing nearby trees when necessary.

Dedication

To Mom, Dad, Kelsie, Kyle, Schwoerer, baby Nora, and little baby Gretta, you guys rock and without your love and support I wouldn't have ever had this opportunity. I'm expecting you all to read this thing cover to cover.

Table of Contents

Abstract	ii
Acknowledgments	iii
Dedication	v
Table of Contents	vi
List of Tables	viii
List of Figures	ix
 Chapter 1: Spatiotemporal Variation of Demographic Parameters: Moose Population Performance	
Across Idaho.....	1
Abstract	1
Introduction	2
Methods	5
Results	13
Discussion	15
Management Implications	21
Literature Cited.....	23
Tables	28
Figures	31
Appendix	39
 Chapter 2: Elevated Winter Tick Burdens: Potential Cost of Seasonal Site Fidelity by Moose.	
Introduction	41
Methods	44
Results	51
Discussion	53
Management Implications	56
Literature Cited.....	57
Tables	62

Figures 66

List of Tables

Table 1.1. Numbers of adult female moose (>1 year of age) and calves (9-10 months of age) fitted with GPS collars across 5 regions in Idaho, USA, 2020-2022.....	28
Table 1.2. Criteria used to specify models of mortality and reproduction for moose in Idaho, USA, during 2020-2022.....	28
Table 1.3. Proportional contribution of demographic parameters (elasticity) to proportional changes in population growth of moose in Idaho, USA, 2020-2022.....	28
Table 1.4. Sample sizes used to estimate adult female mortality and reproduction of moose within 5 regions in Idaho, USA.....	29
Table 1.5. Mean demographic rates reported for moose populations across the southern extent of their range in North America, 1992-2022.....	30
Table 2.1. Descriptions of covariates used to model spring resource selection by moose in Idaho, USA, 2020-2022. Data from both sources (National Land Cover Database, NLCD, and a digital elevation model, DEM) were at a 30 m resolution.....	62
Table 2.2. Numbers and proportions of GPS locations of adult female moose within each National Land Cover Database (NLCD) cover type by study region, in Idaho, USA, during 15 March – 15 May of 2020-2022.....	62
Table 2.3. Top models of spring resource selection by adult female moose at the broad scale for each of six regions in Idaho, USA. Values are reported for number of model parameters (k), model weight (ω_i), and delta Akaike's Information Criterion (ΔAIC).....	63
Table 2.4. Top models of spring resource selection by adult female moose at the local scale for each of six regions in Idaho, USA. Values are reported for number of model parameters (k), model weight (ω_i), and delta Akaike's Information Criterion (ΔAIC).....	64
Table 2.5. Models predicting relative burden of winter ticks as a function of use of the tick risk landscape for moose in 6 study regions across Idaho, USA, 2020-2022. Values are reported for maximized log-likelihood ($\log(L)$), Akaike's Information Criterion (AIC_c), Nagelkerke's pseudo R^2 , delta AIC_c (ΔAIC_c), and AIC weight (ω_i).....	64
Table 2.6. Coefficient estimates and 90% confidence intervals from the top-ranked model for predicting relative tick burden on moose as a function of use of the tick risk landscape in Idaho, USA, 2020-2023. Beta estimates (β) for tick count bins (low, medium, high) can be interpreted as the log odds of moving from one bin to the next based on a one unit increase in tick risk value..	65

List of Figures

- Figure 1.1.** Study regions in Idaho, USA. Circles represent all GPS locations from collared adult female moose during 2020-2023..... 31
- Figure 1.2.** Example of a parturition movement from a GPS collared female moose. A) Speed of movement (m/hr) estimated from the distance between GPS locations recorded at 4-hr intervals across 6 days in May. A birth event signified by the sharp increase in speed (~May 20th) followed by a substantial decrease in movements (~May 21st). B) The same birth movement sequence illustrated across the landscape with lines connecting consecutive GPS locations..... 32
- Figure 1.3.** Weekly mortality rates of adult female moose (curved line), relative to calendar date in Idaho, USA, 2020-2023. Symbols represent proximate causes of mortality. 33
- Figure 1.4.** Histogram of dates of calving by adult female moose collared in Idaho, USA, 2020-2022. 33
- Figure 1.5.** Mean parturition rate (\pm 95% credible interval) for adult female moose captured or not within 6 months prior to the parturition window (~15 May - 15 June). Parturition was modeled separately for individuals in capture year and non-capture year..... 34
- Figure 1.6.** Frequency plots of modeled population growth rates for moose in Idaho, USA, based on three variance models: spatial (black), temporal (red), and spatiotemporal (blue) models. Data represent statewide population growth based on demographic rates estimated in 5 regions across 3 years. Also, within each panel, the mode, 10%, and 90% quantiles, are specified for each of the three variance models as follows: $\lambda = mode [10\% \text{ quantile}, 90\% \text{ quantile}]$ 35
- Figure 1.7.** Results of Life Stage Simulation Analysis (LSA) for moose populations in Idaho, USA. Plot is subset into four panels, corresponding to the four demographic rates estimated during the study (parturition rate, adult female survival, twinning rate, summer calf survival. Within each panel, black dots represent the relationship between the parameter value and the corresponding population growth rate. Also, within each panel is the R^2 value (LSA value) for each demographic rate..... 35
- Figure 1.8.** Estimated demographic rates by region and year for moose in Idaho during 2020-2022. 36
- Figure 1.9.** Frequency plots of demographic rates for moose in Idaho, 2020-2022, by variance model. Demographic rates include annual adult female survival (A), parturition rate (B), twinning rate (C), and summer calf survival (D). Within each panel the colored lines represent the distributions for each of the 3 variance models: spatial (black), annual (red), and spatiotemporal (blue) models. Also, within each panel, the mode, 10%, and 90% quantiles, are specified for each of the three variance models: $model = mode [10\% \text{ quantile}, 90\% \text{ quantile}]$ 36

Figure 1.10. Frequency plots of demographic rates for moose in Idaho, 2020-2022, within each variance model: spatial (A), temporal (B), and spatiotemporal (C)..... 37

Figure 1.11. Birth sites from collared female moose in Idaho, USA. Photographs show a GPS collared adult female with a newborn calf (A), expelled placenta within a birth site, (B) and typical birth site with matted down vegetation and soil with amniotic fluid (C). 38

Figure 1.12. Results of Life Stage Simulation Analysis (LSA) from the temporal model. Plot is subset into four panels, corresponding to the four demographic rates estimated during the study (parturition rate, adult female survival, twinning rate, summer calf survival. Within each panel, black dots represent the relationship between the parameter value and the corresponding population growth rate. Also, within each panel is the R² value (LSA value) for each demographic rate..... 39

Figure 1.13. Results of Life Stage Simulation Analysis (LSA) from the spatial model. Plot is subset into four panels, corresponding to the four demographic rates estimated during the study (parturition rate, adult female survival, twinning rate, summer calf survival. Within each panel, black dots represent the relationship between the parameter value and the corresponding population growth rate. Also, within each panel is the R² value (LSA value) for each demographic rate..... 39

Figure 1.14. Frequency plot of values used for annual calf survival in 3 separate LSAs. The red solid line represents values used in Lehman et al (2018), the green dotted line represents values used in the primary LSA for this study, and the blue dashed line represents values used in the additional LSA for this study and were simulated based on an unrealistically high amount of variation in overwinter calf survival..... 40

Figure 1.15. Life Stage Simulation Analysis (LSA) results for moose populations in Idaho, USA. Plot is subset into five panels, corresponding to the five demographic rates estimated during the study (parturition rate, adult female survival, twinning rate, summer calf survival, and winter calf survival). Within each panel, black dots represent the relationship between the parameter value and the corresponding population growth rate. Also, within each panel is the R² value (LSA value) for each demographic rate. Winter calf survival was simulated to represent an unrealistically high amount of variation for this parameter. 40

Figure 2.1. Study regions (polygons) and GPS locations (circles) used to model spring habitat selection by adult female moose within each region in Idaho, USA, 2020-2022. 66

Figure 2.2. Specificity vs. sensitivity plots of the final predictions of spring moose habitat (AUC=; 0.70-0.92) by study region in Idaho, USA, 2020-2022. 67

Figure 2.3. Parameter estimates (\pm 95% CI) from the top broad-scale models of spring resource selection by adult female moose in six regions of Idaho, USA, 2020-2022.	68
Figure 2.4. Parameter estimates (\pm 95% CI) from the top local-scale models of spring resource selection by adult female moose in six regions of Idaho, USA, 2020-2022.	68
Figure 2.5. Tick risk landscapes estimated as the relative probability of use of habitat by adult female moose during the spring winter tick drop-off period in six study regions in Idaho, USA, 2020-2022.....	69
Figure 2.6. Regional tick risk landscapes estimated as the relative elative probability of selection of habitat by adult female moose during the spring winter tick drop-off period in six study regions in Idaho, USA, 2020-2022. Locations of GPS collared females during the fall tick pick-up period are represented by circles.	70
Figure 2.7. Predictions from the top model for predicting relative winter tick burden on moose as a function of use of the tick risk landscape across 6 study regions in Idaho, USA, 2020-2022. Moose were more likely to acquire a high tick load with increased exposure to the tick risk landscape.	71
Figure 2.8. Annual estimated exposure of moose to the tick risk landscape in Idaho, USA, 2020-2022. Dots represent individual tick risk values for 1-3 years for which data were available, with black lines connecting individuals across years. For individuals with 2-3 years of fall location data, the coefficient of variation ($n = 50$, mean = 0.05) did not differ significantly from zero (p -value = 0.03), indicating comparable exposure to the winter tick risk landscape across years.	72

Chapter 1: Spatiotemporal Variation of Demographic Parameters: Moose Population Performance Across Idaho.

Abstract

Hunter harvest and aerial survey data suggest that some moose populations in Idaho have been declining since the mid-1990s. However, longitudinal demographic data spanning the range of moose in Idaho are lacking, making it difficult to explain observed trends. We quantified spatiotemporal variation in demographic parameters for moose populations across the range of habitats occupied by moose in Idaho during 2020-2022. We fitted 148 adult females and 17 9-month-old calves with GPS collars in 5 study areas and used the resulting data to estimate survival. To document calf production and calf survival through summer, we observed parturient collared females during 15 May – 31 August. We used a hierarchical Bayesian framework to estimate survival and reproductive rates. We then used a life stage simulation analysis (LSA) to explore how these demographic parameters influenced growth of moose populations. Elasticity values indicated that population growth was more sensitive to changes in adult female survival than to all other vital rates combined. Results of the LSA suggested that variation in survival of adult females strongly influenced observed trends in moose populations across Idaho. These analyses provide the first statewide demographic assessment for moose in Idaho, help to identify key life stages for future research and management, and lay the foundation for evaluating the ecological factors contributing to population declines. Results from this study can help guide moose management and research in Idaho and contribute more broadly to an understanding of moose population dynamics across changing landscapes in the western USA.

Introduction

Wildlife population dynamics are a product of complex interactions among multiple demographic rates and a variety of extrinsic factors. Some demographic rates have a disproportionate influence on population growth (λ) and understanding the relative contributions of different vital rates to λ is critical for optimizing population management strategies (Gaillard et al. 2000, Becker et al. 2010, Johnson et al. 2010). In ungulates, prime-aged adult females typically are the main contributors to population growth through reproduction (Gaillard et al. 1998). Additionally, adult females are usually more resistant to common mortality factors than young or senescent age classes (Loison et al. 1999, Gaillard and Yoccoz 2003, Owen-Smith and Mason 2005), which commonly results in adult survival being high and stable across time and space (Pfister 1998). Because adult survival has a stronger influence on population growth, even small deviations in this vital rate can impact populations to a much greater degree than other demographic rates (Oates et al. 2021). Conversely, although juveniles contribute less to population growth via reproduction, they often experience lower and more variable survival than adults (Gaillard et al. 2000, Delgiudice et al. 2007, Horne et al. 2019). Consequently, variation in juvenile survival is often a better predictor of annual changes in population abundance (Gaillard et al. 1998, Raithel et al. 2007, Paterson et al. 2019).

Elasticity quantifies the proportional contribution of different demographic parameters to population growth (de Kroon et al. 1986). However, one limitation to interpreting elasticity is that the calculations ignore spatiotemporal variation in demographic rates (Wisdom et al. 2000). If demographic rates vary across gradients of predator or parasite densities, habitat quality, or severity in annual weather patterns, management actions can be directed to improve those rates. Conversely, if those demographic rates are invariable across

those same spatiotemporal gradients, improving habitat quality or reducing predator and parasite densities would do little to improve demographic performance. Combining measures of elasticity and variability holds potential to help identify demographic rates that both influence overall population size and those that management actions have the ability to change (Wisdom et al. 2000).

In recent decades, declines in moose populations have been documented across the southern extent of their range in North America (Wattles and DeStefano 2011, DeCesare et al. 2012, Mech and Fieberg 2014, Nadeau et al. 2017). These declines have been attributed to a suite of factors including predation, parasites, disease, and changes in habitat quality (Severud et al. 2019, Ellingwood et al. 2020), all of which can affect reproduction and survival of different age classes in diverse ways (Murray et al. 2006, Samuel 2007, Schrempf et al. 2019). For example, in the northeastern USA, researchers estimated that winter tick (*Dermacentor albipictus*) infestation was primarily responsible for overwinter calf mortality rates of nearly 70% across multiple years (Jones et al. 2019). Meningeal worm (*Parelaphostrongylus tenuis*) has also been identified as an important pathogen driving population dynamics in Minnesota, but it only affects older age classes (Murray et al. 2006). In Utah, researchers found that maternal fat stores were correlated with reproductive output of multiple moose populations (Ruprecht et al. 2016), linking reproductive effort to habitat quality. Moose populations across the southern periphery of their range in North America experience numerous stressors that impact reproduction and survival. Identifying these stressors and understanding how they shape demographic performance and population growth is a critical area of research for wildlife agencies attempting to understand and manage declining populations.

The distribution of moose in Idaho spans a diversity of climate regimes and habitat types that produce spatial heterogeneity in forage availability and quality, thermal regimes, and densities of competitors, predators, and parasites. Moreover, variation in precipitation, temperature, and anthropogenic or natural disturbances can contribute to a complex landscape of risk for moose populations across the state. Understanding how such variation influences demographic rates and population growth could help elucidate mechanisms influencing performance of moose populations. Hunter harvest records and aerial survey data suggest that moose have been declining across portions of their range in Idaho since the mid-1990s (Nadeau et al. 2017, Schrempp et al. 2019, Idaho Department of Fish and Game 2020); however, demographic data that span the range of moose in Idaho are lacking.

The goal of this study was to estimate demographic rates for moose populations throughout Idaho and to incorporate spatial and temporal variation in demographic parameters into models of population growth. We addressed two management-relevant questions: (1) How do demographic rates of moose in Idaho compare to other populations in North America? and (2) Which demographic rates account for the most variation in population growth of moose populations in Idaho? We estimated survival and reproduction of GPS collared moose during 2020-2022 within five study regions across Idaho. We then used stochastic population modeling to evaluate spatial and temporal variation in demographic parameters and population growth among study regions and years. We predicted that population growth would be most sensitive to variation in adult female survival. Furthermore, we predicted that variation in population growth would be strongly influenced by annual calf recruitment across all study regions. Results from this study can help guide moose management and research in Idaho and contribute more broadly to an

understanding of moose population dynamics across changing landscapes in the western USA.

Methods

Study Regions – This study was conducted in 5 regions in Idaho, USA that were selected to represent the majority of variation in moose habitat and harvest management strategies within the state (Fig. 1.1). Our study area encompassed three major ecoregions that are characterized by diverse habitat types, predator complexes, and densities of moose and other ungulates.

The Selkirk region, which is contained within the Northern Rockies ecoregion, is characterized by high topographic relief and elevations ranging from 450 to 2,300 m. This area is dominated by mixed coniferous forest, with common tree species including grand fir (*Abies grandis*), western red cedar (*Thuja plicata*), western hemlock (*Tsuga heterophylla*), larch (*Larix occidentalis*), and white pine (*Pinus strobus*). This area experiences high annual precipitation ranging from 56 to 140 cm per year, with mean monthly temperatures ranging from -9 to 30 °C (NCDC 2020).

Also contained within the Northern Rockies ecoregion is the Clearwater region. The topography of this region ranges from gently sloping hills to steep mountains, with elevations of 450-2,000 m, annual precipitation from 61 to 165 cm, and mean monthly temperatures ranging from -7 to 28 °C (NCDC 2020). Dominant tree species include western red cedar, western hemlock, and white pine, with intensive logging occurring across much of the region.

The Lost River region, located in the Middle Rockies ecoregion, is extremely topographically diverse with low-elevation valley floors dominated by grass and shrubland species and high-elevation alpine and montane environments dominated by western spruce

(*Picea sitchensis*), Douglas fir (*Pseudotsuga menziesii*), and lodgepole pine (*Pinus contorta*). Elevations range from 1,158 to 3,859 m, mean annual precipitation ranges from 15 to 112 cm, and mean monthly temperatures range from -17 to 29 °C (NCDC 2020).

The Bannock region is located within the Northern Basin and Range ecoregion, with elevations ranging from 900 to 2,700 m, mean annual precipitation from 20 to 76 cm and mean monthly temperatures from -13 to 29 °C (NCDC 2020). This region is dominated by multiple tree species including western spruce, Douglas fir, lodgepole pine, and bigtooth aspen (*Populus grandidentata*).

The Island Park region is also situated within the Middle Rockies ecoregion, with dominant tree species including Douglas fir and lodgepole pine interspersed with shrub steppe habitat dominated by sagebrush (*Artemisia* spp.). The Island Park region is located at higher elevation (1,500-2,900 m) and experiences annual precipitation between 15 and 102 cm and mean temperatures ranging from -17 to 31 °C (NCDC 2020).

Animal Capture – We captured adult female moose and 9-month-old calves between January and March of 2020 and 2021. All moose were darted from a helicopter and fitted with global position system (GPS) collars (G5-2D Iridium, Advanced Telemetry Systems, Isanti, MN, USA) that were programmed to drop off ~2 years after deployment for adults and ~6 months for calves. All collars were programmed to record a location every 4 hours, transmit locations to a satellite twice per day, and send an email notification if stationary for > 6 hours, signaling a mortality event. For all captured moose, we collected approximately 20 ml of blood via jugular venipuncture and collected standard morphological measurements (i.e., chest girth, body length, hind foot length). Blood samples from adult females were later centrifuged to separate serum and analyzed for protein-specific B (PSPB) by

radioimmunoassay to detect pregnancy status. All capture and animal handling procedures were conducted under the approval of the University of Idaho Institutional Animal Care and Use Committee (IACUC protocol 2020-17) and in compliance with guidelines for use of wild mammals in research (Sikes et al. 2016).

Monitoring parturition and neonate survival – Adult females were monitored during May and June to document parturition events and the presence of neonates. GPS locations and movement rates were analyzed daily using visual inspection to discern movements associated with births such as an irregular, long distance movement followed by a localization (Fig. 1.2). These movements were flagged as possible birth events and investigated within 24-48 hours, either by an observer on foot using VHF telemetry or in a fixed-wing plane using infrared technology, to locate the female and inspect the area for the presence of neonates. Cow-calf pairs were relocated every 30 days until September using ground-based methods to monitor survival of calves through summer. We assumed that calves were dead if we relocated the dam but did not observe the calf or calves at heel. We only recorded a calf death if we attained an unobstructed view of the dam and her surrounding area. If a calf death was recorded, at least one additional attempt was made to observe the female again before the end of the summer to confirm calf mortality. During these subsequent observations ($n=32$), we never detected a calf-at-heel with the dam.

Mortality & Reproductive Models – We used a hierarchical Bayesian framework to model mortality and reproduction across years and regions of our study (Lehman et al. 2018, Horne et al. 2019).

Adult female mortality was estimated using a known fate approach with weekly time steps from June 1 to May 31 of the following year. Although no moose were monitored

during calendar year 2019, study year 2019 spanned June 2019 – May 2020. We assumed adult mortality was a Bernoulli random variable with weekly mortality probability, $p_{t,y,s}$:

$$d_{t,y,s} \sim \text{Bern}(p_{t,y,s})$$

where $d_{t,y,s} = 1$ if an individual died within week t , year y , and population s , and 0 otherwise.

We then assumed a logit-linear model for weekly mortality with a 3-knot cyclic spline function to allow for intra-annual changes in mortality probability:

$$\begin{aligned} \text{logit}(p_{t,y,s}) &= \text{spline}_{t,y,s} \\ \text{spline}_{t,y,s} &= \beta_{0,y,s} + \beta_1 \times X2_t + \beta_2 \times X3_t \end{aligned}$$

We made the following assumptions about spatiotemporal variation in adult female mortality:

$$\beta_{0,y,s} \sim \text{Normal}(\mu_{y,s}, \sigma_y)$$

$$\mu_{y,s} \sim \text{Normal}(\mu_s, \sigma_y)$$

$$\mu_s \sim \text{Normal}(\mu, \sigma_s)$$

Annual adult female survival (S_a) was then calculated as the product of 1 minus weekly mortality rates:

$$S_a = \prod (1 - p_{t,y,s})$$

Summer calf mortality was estimated from birth to 60-days post birth for each individual. We assumed survival of calves during summer was a Bernoulli random variable:

$$Y_{i,c} \sim \text{Bern}(p_{i,c})$$

Where $p_{i,c}$ represents the probability of death for each individual (i) during the interval from $t_{i,c-1}$ to $t_{i,c}$. Where (c) represents the occasion when a calf was checked and (t) represents time

in days. Furthermore, $Y_{i,c} = 0$ if the calf is seen with the cow and 1 otherwise (indicating mortality sometime between the last check and the current check).

Thus,

$$p_{i,c} = 1 - \frac{S(t_c)}{S(t_{c-1})}$$

where $S(t)$ is the probability of surviving to time t .

We further assumed a Weibull survival model (Carroll 2003) to allow for changes in the probability of mortality with age using shape parameter a and scale parameter b .

$$S(t) = \exp\left[-\left(\left(\frac{t}{b}\right)^a\right)\right]$$

Thus,

$$p_{i,c} = 1 - \frac{\exp\left[-\left(\left(\frac{t_c}{b}\right)^a\right)\right]}{\exp\left[-\left(\left(\frac{t_{c-1}}{b}\right)^a\right)\right]} = 1 - \exp\left[\frac{-(t_c^a) + t_{c-1}^a}{b^a}\right]$$

For estimation, we reparametrized the Weibull distribution in terms of overall survival rate for 60 days (S_{60}) using $b = 60/(-\ln(S_{60}))^{1/a}$. Thus, the probability of survival during a time interval was a function of 2 parameters, the overall survival rate, S_{60} , and the shape of the survival curve, a . Spatiotemporal variation in survival was assumed to affect the overall survival rate while the shape parameter was assumed to be constant. Thus,

$$\begin{aligned}\text{logit}(S_{60_{y,s}}) &= \mu_{calf_{y,s}} \\ \phi_{calf_s} &\sim \text{Normal}(\theta_{calf}, \sigma_{calf_s}) \\ \mu_{calf_{y,s}} &\sim \text{Normal}(\phi_{calf_s}, \sigma_{calf_y})\end{aligned}$$

Where $\text{logit}^{-1}(\phi_{calf_s})$ is the expected 60-day survival rate for each population s , and

σ_{calf_y} measures the annual variation within a population. Furthermore,

$\text{logit}^{-1}(\theta_{_calf})$ is the expected 60-day survival rate across all populations, and $\sigma_{_calf_s}$ measures the spatial variation across populations.

We estimated adult female reproduction as a function of parturition rate ($\theta_{_p_{y,s}}$; number of parturient adult females per total adult females) and twinning rate ($\theta_{_t_{y,s}}$; probability twins are born per parturient adult female). The expected number of calves born per adult female (N_c) is then

$$N_c = \theta_{_p_{y,s}} \times (1 + \theta_{_t_{y,s}}).$$

We modeled parturition and twinning using similar models and assumed these parameters were Bernoulli random variables where $Z_{y,s} = 1$ if an individual adult female in population s and year y gave birth, and 0 otherwise and $C_{y,s} = 1$ if a parturient adult female in population s and year y gave birth to twins, and 0 otherwise. Thus,

$$Z_{y,s} \sim \text{Bern}(\theta_{_p_{y,s}})$$

and

$$C_{y,s} \sim \text{Bern}(\theta_{_t_{y,s}})$$

We then assumed a logit-linear model for parturition and twinning:

$$\text{logit}(\theta_{_ \cdot_{y,s}}) = \mu_{_ \cdot_{y,s}}$$

We made the following assumptions about spatiotemporal variation in parturition and twinning:

$$\mu_{_ \cdot_{y,s}} \sim \text{Normal}(\mu_{_ \cdot_s}, \sigma_{_ \cdot_y})$$

$$\mu_{_ \cdot_s} \sim \text{Normal}(\mu_{_ \cdot}, \sigma_{_ \cdot_s})$$

We fit all survival and reproductive models using Bayesian Markov Chain Monte Carlo (MCMC) methods with model specific criteria provided in Table 1.2. We assumed

vague prior distributions for all population-level mean and variance parameters. For all models we ran 3 chains, using trace plots to determine sufficient burn-in and convergence ($\hat{R} \leq 1.1$; Gelman et al. 2014). Models were fit in Program R version 4.2.2 (R Core Team, 2022) using JAGS software (version 4.3.1; Plummer 2003) and the R package JagsUI (version 1.5.2; Kellner 2021).

Population Growth -- To estimate asymptotic population growth rates (λ) and covariate elasticities (E ; proportional change in λ resulting from a change in each demographic rate), we inputted estimates of survival and reproduction into a post-birth, female-based matrix model (Caswell 2001) that took the following form:

$$A = \begin{bmatrix} 0 & 0 & (S_a * \frac{\theta_{-p_{y,s}} * (\theta_{-t_{y,s}} + 1)}{2}) \\ S_{cs} * S_{cw} & 0 & 0 \\ 0 & S_y & S_a \end{bmatrix}$$

where S_a and S_y are annual survival for adult females and yearlings, respectively. $\theta_{-p_{y,s}}$ and $\theta_{-t_{y,s}}$ are the parturition rate and twinning rate for adult females (as females born per adult female, assuming a 1:1 sex ratio), and S_{cs} and S_{cw} are calf survival during summer and winter, respectively. Asymptotic population growth (λ) was calculated as the dominant eigenvalue of matrix A . Elasticity (E) of each demographic rate within matrix A was calculated following Caswell (2001) and Morris & Doak (2002). Because we did not monitor yearling survival, we estimated a yearling survival rate from the literature, which on average was 7% below adult survival (Oates et al. 2021).

To estimate variation in population growth, we randomly drew 10,000 sets of demographic rates from the models described above. Specifically, we estimated the effect of

spatial (s), temporal (y), and spatiotemporal (sy) variance on each demographic rate (D) by simulating 3 distributions for each rate, using corresponding mean and variance components:

$$D_s \sim \text{Normal}(\hat{\mu}, \hat{\sigma}_s)$$

$$D_y \sim \text{Normal}(\hat{\mu}, \hat{\sigma}_y)$$

$$D_{sy} \sim \text{Normal}(D_s, \hat{\sigma}_y)$$

where $\hat{\mu}$ is the estimate for each of the statewide demographic rates (calculated as the mode of the posterior of μ in the models described above), and $\hat{\sigma}_s$ and $\hat{\sigma}_y$ are the estimates for spatial and annual variance for each of the statewide demographic rates (calculated as the mode of the posteriors of σ_s and σ_y in the models described above). With each set of demographic rates, we created a matrix replicate of the form (A_r), from which we calculated λ_r and E_r . For each matrix replicate, yearling survival was calculated as: $Sy_r = Sa_r - 0.07$, and over-winter calf survival was held at a constant 0.52.

Life Stage Simulation Analysis- We used a life-stage simulation analysis (LSA; Wisdom et al. 2000) to identify demographic rates that caused spatiotemporal variation in population growth by regressing λ on each demographic rate. Because yearling survival was estimated from the literature and over-winter calf survival was held at a constant value, we do not report values for these parameters from this LSA. However, because over-winter calf survival is typically highly variable, we ran an additional LSA where we simulated an unrealistically high amount of variation for overwinter calf survival which is outside of reported values from other studies on ungulates in North America. The additional LSA was conducted to compensate for our lack of overwinter calf survival data and will illustrate the effect of this parameter on population trends even if it was beyond the normal bounds of variation.

Results

We captured 148 adult female moose during 2020-2021 (Table 1.1). A subset of collars fitted on adult females failed within one year after deployment ($n = 32$; average days online = 195), and we right censored those individuals before the end of the study period. We assumed that collar failure was independent of mortality and that the fate of right-censored individuals was representative of the parameter estimate for adult female mortality.

Annual mortality of adult females in our study was low and relatively consistent across regions and years. We modeled mortality of adult females using 23 mortalities from 148 individuals (390 moose-years), and the resulting estimate was 0.09 (95% credible interval = 0.05-0.19). Weekly mortality of adult females peaked in late April and was lowest during the summer and fall months (Fig. 1.3). Cause-specific mortality of collared adult females was attributed to diverse proximate factors: vehicle collision ($n = 3$), train collision ($n = 1$), winter tick/emaciation ($n = 5$), bacterial infection ($n = 5$), carotid artery worm ($n = 3$), fall ($n = 1$), and unknown ($n = 5$) (Fig. 1.3).

Calf mortality varied across the annual cycle. Summer calf mortality (0-60 days postpartum) was modeled using 54 mortalities from 186 calves, and the resulting estimate was 0.35 (95% credible interval = 0.28-0.43). In contrast, estimated mortality of calves during winter was moderate (0.47). This rate, however, was estimated from a relatively small sample size of animals collared at 9-10 months of age ($n = 17$). We were not able to estimate spatiotemporal variation in winter calf mortality because calves were collared only for one year and across only 3 of the 5 study regions. Most mortalities (5 of 8) occurred between mid-April and early May, and proximate causes included winter tick/emaciation ($n = 5$), vehicle collision ($n = 1$), wolf predation ($n = 1$), and bacterial infection ($n = 1$).

Reproduction of adult females was relatively high and consistent among years (Fig. 1.8). The annual pregnancy rate during 2020 and 2021 was 89%. The majority (87%) of calves were born between May 17 and June 1 of each year (Fig. 1.4) and using movements of collared females to detect parturition events, we were able to locate and observe >75% of calves within 24-48 hours after birth (based on mobility of the calf and/or timing of localization of the dam). During parturition observations, we commonly found evidence of a birth site, including a larger than normal bed-site (~2x2 m area with matted down vegetation or disturbed soil, amniotic fluid, blood, and placental tissue; Fig. 1.11). We also found 3 calves dead at the birth site.

We modeled parturition and twinning rates using 160 births from 140 adult females (235 moose-years; Table 1.4), which resulted in 186 total calves and 26 sets of twins. The parturition rate was 0.85 (95% credible interval = 0.76-0.92) and the twinning rate was 0.14 (95% credible interval = 0.06-0.24). Both reproductive parameters differed more among regions than between years (Fig. 1.9). We also noted a difference in parturition rates between moose that were captured within 6 months prior to the parturition window (~May – June) and those that were not (Fig. 1.5). Based on pregnancy determination at the time of capture, 33% (40/121) of pregnant females were never observed with a calf in the subsequent spring. We accounted for the potential effect of capture year on parturition by adding an interaction term between capture year and probability of parturition into our reproductive model. The relatively high overall estimate of reproduction suggests that any effects of capture were unlikely to have influenced estimates of population growth.

Necropsies from 2 of the 3 calves found dead at their birth site revealed that complications during birth may have been the reason for mortality. Furthermore, three adult

cows were observed with a retained placenta after parturition, and one subsequently died from internal hemorrhaging and infection. Collectively, these results suggest that reproductive challenges associated with parturition may have influenced the rates of survival and reproduction documented in this study.

Simulating combinations of demographic rates within our projection matrix resulted in an asymptotic population growth rate of 1.05 (10 and 90% quantile = 0.90-1.08). Based on the three separate models of variation (spatial, temporal, and spatiotemporal), population growth was most influenced by the combined effects of spatial and temporal variation (Fig. 1.6). As expected, elasticity values indicated that population growth was more sensitive to changes in adult female survival ($E = 0.83$, 10 and 90% quantile = 0.80-0.87) than to all other demographic rates combined ($E = 0.35$, 10 and 90% quantile = 0.28-0.42; Table 1.3).

The life stage simulation analysis (LSA) indicated that observed variation in population growth could be explained almost entirely by variation in adult female survival ($R^2 = 0.95$) relative to all other demographic rates combined ($R^2 = 0.05$). LSA values differed slightly among the 3 variance models, but adult female survival remained highly correlated with population growth in all 3 models (Appendix; Fig. 1.12-1.13). Furthermore, the additional LSA indicated even if overwinter calf survival was more variable than values reported elsewhere, adult female survival would still explain the majority of variation in population growth (Appendix; Fig. 1.13-1.14).

Discussion

Our results indicate that statewide, the moose population in Idaho was relatively stable during the study period. However, among regions and years, annual population growth fluctuated around 1.0 (mean=1.05, 10 and 90% quantiles = 0.90-1.08). Although the overall annual mortality estimate for adult females was low (0.09), spatiotemporal variation in adult

mortality was primarily responsible for variation in population growth across space and time. In contrast, reproduction and annual calf recruitment did not influence population growth as strongly as adult survival, although both parameters still contributed to the observed spatiotemporal variation in population growth. Adults and calves experienced diverse mortality factors, with winter tick infestation and associated emaciation being relatively common among GPS-collared individuals of both age classes. Expanding understanding of factors influencing spatiotemporal variation in adult female mortality, as well as the combined influence of other demographic rates, will improve our understanding of moose population dynamics in Idaho and other populations across the southern extent of their range in North America.

Although modest in magnitude, variation in adult female mortality among regions and years contributed to observed mortality rates for adult females, which strongly influenced our estimates of population growth. Fluctuations in annual weather patterns likely influence mortality of ungulates indirectly through effects on forage, diseases, and predators, and directly through energy costs associated with thermoregulation or locomotion in deep snow. Weather also likely influences survival of moose due to annual responses of winter ticks to summer temperatures (Hoy et al. 2021) and variation in precipitation during summer and late winter (Drew and Samuel 1986, Samuel 2007, Debow et al. 2021). Similarly, mortality of adult female elk increased with winter precipitation specifically in areas of high predator densities, through malnutrition and poor ability to evade predators (Brodie et al. 2013). Nutritional condition and annual and late winter precipitation have also been tied to mortality of adult female mule deer (Bender et al. 2007). These studies suggest that although proximate causes of mortality for adult female ungulates may be diverse, the underlying driver is often

seasonal and annual weather cycles that decrease fitness and make animals more vulnerable to predation, disease, and malnutrition. Furthermore, across our study regions, moose experience variable habitat types and densities of predators, parasites and other ungulates creating a spatially heterogeneous landscape of risk. Predicting responses of adult females to both spatial and annual variation in mortality factors will be critical for assessing future population trends of moose in Idaho.

Mortality of calves over summer was more strongly influenced by annual variation than spatial variation, suggesting that annual changes in environmental factors may be influencing survival of calves. High infestation levels of winter ticks within populations can reduce survival of offspring during the year following an epizootic (Jones et al. 2017). This is likely a result of highly infested adult females experiencing reduced nutritional condition during late gestation, giving birth to smaller calves, and having less endogenous resources to pass on to their young through lactation and maternal care (Jones et al. 2017). We assumed that predator densities did not differ markedly among the years of our study, and instead hypothesize that annual changes in weather patterns, forage quality and winter tick infestations created cascading effects on population dynamics, which manifested in the temporally variable summer calf survival rates documented in our study.

In contrast to calf survival, both parturition and twinning were affected more by spatial variation than annual variation, suggesting that regional differences in habitat quality and/or population density could be influencing reproduction more than annual fluctuations in environmental factors. Although the LSA indicated that spatiotemporal variation in reproduction did not strongly affect population growth, understanding factors influencing

reproduction across our study regions could contribute to knowledge of population trends observed in the state.

Our study spanned multiple ecoregions and encompassed broad environmental gradients, which likely contributed to spatial variability in demographic rates. For example, the Clearwater region consistently had lower mortality rates and higher reproductive rates across most years than other regions. (Fig. 1.8). This disparity could stem from several factors, but most notably this region experiences more extensive logging than all other regions. The regeneration of early successional growth following timber harvest can improve forage availability and quality (Visscher and Merrill 2009, Schrempp et al. 2019) and may even buffer moose from predators and parasites (Collins and Schwartz 1998). The Selkirk region has similar habitat composition, predator communities, and climate regimes, but we documented lower reproductive rates and higher mortality rates there than in the Clearwater. However, moose in the Selkirk region tend to exhibit seasonal movements that could influence access to forage during late winter and also increase transmission of parasites and diseases, especially winter ticks (Chapter 2, Proffitt et al. 2016). Wolves also occur in the Selkirk region, and although predation was not a major determinant of adult mortality in our study, the risk of predation could push moose into sub-optimal habitats, with decreased forage quality and thermoregulatory properties (Kie 1999, Becker et al. 2010). Our data suggest that reproduction and survival were at or below average in the Bannock region, which experiences lower summer precipitation than the other regions, and this more xeric environment could result in lower forage quality or quantity relative to the other regions in our study. Documenting spatial variation in predator densities, forage quality, and seasonal

ranges could help identify region-specific management practices to improve moose populations throughout the state.

The mean demographic rates we documented for moose in Idaho were at or above those reported for other moose populations across the southern extent of their range in North America. Our estimates of adult female survival and reproduction were generally higher, and survival of calves comparable, to rates in other published studies (Table 1.5). These high demographic rates combined to produce a relatively stable population growth rate. Nevertheless, modest variation in adult female survival still led to variation in predicted population growth among regions and years.

Because adult female survival was a highly elastic parameter, even slight deviations from the mean value impacted population growth markedly more than other demographic rates. The results of our LSA are likely a product of highly elastic and slightly variable annual survival of adult females and low spatiotemporal variation in the remaining demographic rates. A recent study conducted in Wyoming also reported that adult female survival was the demographic rate that most influenced population growth (Oates et al. 2021). This may indicate that Shiras moose in general experience more variable adult female survival compared to other subspecies across North America, resulting in a relatively high impact on population growth. Understanding the factors driving adult female survival across moose populations in the western USA could inform strategies for reversing negative population trends.

Elasticity analyses conducted on other ungulate populations similarly identified that adult female survival was the most elastic or important demographic rate (Raithel et al. 2007, Johnson et al. 2010, DeCesare et al. 2012, Lehman et al. 2018). In contrast to our results,

these same studies also commonly reported that calf or juvenile recruitment was the parameter most strongly correlated with population growth (Raithel et al. 2007, DeCesare et al. 2012, Lehman et al. 2018). This disparity could stem from several factors. First, our dataset lacked the necessary sample size to attain accurate parameter estimates and variances for overwinter calf survival. Because overwinter survival of moose calves was more variable than summer calf survival in other populations (Jones et al. 2017, 2019), we likely underestimated the amount of spatiotemporal variation in annual calf recruitment. However, the additional LSA indicated that even if overwinter calf survival was more variable than values reported elsewhere, adult female survival would still be a stronger predictor of variation in population growth compared to all other demographic rates. Second, we estimated an annual survival rate for yearling females from the literature and allowed it to track adult female survival within each matrix replicate ($S_{Yr} = S_{Ar} - 0.07$). However, if mean annual survival for yearlings in Idaho is different from other study areas or does not closely track adult survival, then it is possible yearling survival also could affect the results of our LSA.

We observed that reproduction appeared to be lower for adult females captured within 6 months of parturition. Because our overall mean parturition rate was high, we assumed that this difference did not affect our overall estimate of parturition. Field observations of dead calves within birth sites and retained placentas for adult females not in their capture year suggest that environmental stressors may influence reproduction in addition to capture. However, our results still suggest that effects of capture (e.g., immobilization, drug use, stress) could influence reproduction by moose. Vartanian (2012) reported similar results for moose captured and monitored in Wyoming, USA, observing a difference in parturition rates

relative to being ‘handled’ or not within a given calendar year. Our results suggest that research investigating whether and how capture of moose could affect reproduction will be important for the continued monitoring of moose across their range.

Management Implications

Because moose population performance was primarily driven by mortality of adult females, management actions that focus on decreasing mortality of adult females would be most effective for improving population trends across Idaho. However, causes of adult female mortality in our study were diverse, and consequently, it may be difficult to implement management actions that address such a broad set of mortality factors.

Nonetheless, parasites and disease accounted for the largest portion of adult mortality during this study, and focusing on understanding and mitigating these pathogens through land management practices could reduce severity of infections and infestations. In addition, improving habitat within core areas of moose range could decrease annual variation in mortality of adult females. For example, in Idaho and the intermountain west, recent interest in the use of beaver dam analogs (BDA) and the translocation of beavers (*Castor canadensis*) to manipulate and improve habitat may provide a solution to moose populations limited by availability of riparian habitats (Weber et al. 2017). Directing the use of BDAs and beaver translocations within areas where moose are having to travel long distances to acquire the benefits from these habitats could be valuable.

Spatiotemporal variation in annual calf recruitment strongly influences population growth in other ungulate systems (e.g., Lehman et al. 2018, Debow et al. 2021). Expanding our knowledge about variation and causes of winter calf mortality will support a more robust examination of the role of calf recruitment in driving population dynamics of moose in Idaho. Furthermore, investigating the effects of habitat, disease, and parasites, specifically

winter ticks, on moose demography in Idaho, could reveal mechanisms that affect both survival and reproduction of moose, and provide managers with a foundation for developing plans to mitigate their effects on moose populations.

Literature Cited

- Becker, S. A., M. J. Kauffman, and S. H. Anderson. 2010. Nutritional Condition of Adult Female Shiras Moose in Northwest Wyoming. *Alces* 46:151–166.
- Bender, L. C., L. A. Lomas, and J. Browning. 2007. Condition, survival, and cause-specific mortality of adult female mule deer in North-Central New Mexico. *The Journal of Wildlife Management* 71:1118–1124.
- Brodie, J., H. Johnson, M. Mitchell, P. Zager, K. Proffitt, M. Hebblewhite, M. Kauffman, B. Johnson, J. Bissonette, C. Bishop, J. Gude, J. Herbert, K. Hersey, M. Hurley, P. M. Lukacs, S. Mccorquodale, E. Mcintire, J. Nowak, H. Sawyer, D. Smith, and P. J. White. 2013. Relative influence of human harvest, carnivores, and weather on adult female elk survival across western North America. *Journal of Applied Ecology* 50:295–305.
- Carroll, Kevin J. 2003. On the use and utility of the Weibull model in the analysis of survival data. *Controlled clinical trials* 24:682-701.
- Collins, W. B., and C. C. Schwartz. 1998. Logging in Alaska's boreal forest: creation of grasslands or enhancement of moose habitat. *Alces: A Journal Devoted to the Biology and Management of Moose* 34:355–374.
- Coulson, T., J. M. Gaillard, and M. Festa-Bianchet. 2005. Decomposing the variation in population growth into contributions from multiple demographic rates. *Journal of Animal Ecology* 74:789–801.
- Debow, J., J. Blouin, E. Rosenblatt, C. Alexander, K. Gieder, W. Cottrell, J. Murdoch, and T. Donovan. 2021. Effects of winter ticks and internal parasites on moose survival in Vermont, USA. *The Journal of Wildlife Management* 85:1423–1439.
- DeCesare, N. J., M. Hebblewhite, M. Bradley, K. Smith, D. Hervieux, and L. Neufeld. 2012a. Estimating ungulate recruitment and growth rates using age ratios. *Journal of Wildlife Management* 76:144–153.
- DeCesare, N. J., T. D. Smucker, R. A. Garrott, and J. A. Gude. 2012b. Moose status and management in Montana. *Alces* 50:35–51.
- Delgiudice, G. D., M. S. Lenarz, and M. Carstensen Powell. 2007. Age-specific fertility and fecundity in northern free-ranging white-tailed deer: evidence for reproductive senescence? *Journal of Mammalogy* 88:427–435.

- Drew, M., and W. Samuel. 1986. Reproduction of the winter tick, *Dermacentor albipictus*, under field conditions in Alberta, Canada. *Canadian Journal of Zoology* 64:714–721.
- Ellingwood, D. D., P. J. Jones, Henry, Musante, and Anthony R. 2020. Evaluating moose *Alces alces* population response to infestation level of winter ticks *Dermacentor albipictus*.
- Gaillard, J., M. Festa-Bianchet, and N. G. Yoccoz. 1998. Population dynamics of large herbivores: Variable recruitment with constant adult survival. *Trends in Ecology and Evolution* 13:58–63.
- Gaillard, J., M. Festa-Bianchet, N. Yoccoz, A. Loison, and C. Toïgo. 2000. Temporal variation in fitness components and population dynamics of large herbivores. *Annual Review of Ecology and Systematics* 31:367–393.
- Gaillard, J. M., and N. G. Yoccoz. 2003. Temporal variation in survival of mammals: a case of environmental canalization? *Ecology* 84:3294–3306.
- Gelman, A., J. Hwang, and A. Vehtari. 2014. Understanding predictive information criteria for Bayesian models. *Statistics and Computing* 24:997–1016.
- Horne, J. S., M. A. Hurley, C. G. White, and J. Rachael. 2019. Effects of wolf pack size and winter conditions on elk mortality. *Journal of Wildlife Management* 83:1103–1116.
- Hoy, S. R., L. M. Vucetich, R. O. Peterson, and J. A. Vucetich. 2021. Winter tick burdens for moose are positively associated with warmer summers and higher predation rates. *Frontiers in Ecology and Evolution* 9:780.
- Idaho Department of Fish and Game. 2020. Idaho Moose Management Plan 2020-2025.
- Johnson, H., S. Mills, T. Stephenson, and J. Wehausen. 2010. Population-specific vital rate contributions influence management of an endangered ungulate. *Ecological Applications* 20:1753–1765.
- Jones, H., P. J. Pekins, L. E. Kantar, M. O’neil, and D. Ellingwood. 2017. Fecundity and Summer Calf Survival of Moose During 3 Successive Years of Winter Tick Epizootics. *Alces* 53:85–98.
- Jones, H., P. Pekins, L. Kantar, I. Sidor, D. Ellingwood, A. Lichtenwalner, and M. O’neal. 2019. Mortality assessment of moose (*Alces alces*) calves during successive years of winter tick (*Dermacentor albipictus*) epizootics in New Hampshire and Maine (USA). *Canadian Journal of Zoology* 97:22–30.

- Kie, J. G. 1999. Optimal foraging and risk of predation: effects on behavior and social structure in ungulates. *Journal of Mammalogy* 80:1114–1129.
- de Kroon, H., A. Plaisier, J. Van Groenendael, and H. Caswell. 1986. Elasticity: the relative contribution of demographic parameters to population growth. *Ecology* 67:1427–1431.
- Lehman, C. P., C. T. Rota, J. D. Raithel, and J. J. Millspaugh. 2018. Pumas affect elk dynamics in absence of other large carnivores. *Journal of Wildlife Management* 82:344–353.
- Loison, A., M. Festa_Bianchet, J.-M. Gaillard, J. T. Jorgenson, and J.-M. Jullien. 1999. Age-specific survival in five populations of ungulates: evidence of senescence. *Ecological Society of America* 2539–2554.
- Mech, L. D., and J. Fieberg. 2014. Re-evaluating the northeastern Minnesota moose decline and the role of wolves. *The Journal of Wildlife Management* 78:1143–1150.
- Murray, D. L., E. W. Cox, W. B. Ballard, H. A. Whitlaw, M. S. Lenarz, T. W. Custer, T. Barnett, and T. K. Fuller. 2006. Pathogens, nutritional deficiency, and climate influences on a declining moose population. *Wildlife Monographs* 166:1–30.
- Nadeau, M. S., N. J. Decesare, D. G. Brimeyer, E. J. Bergman, R. B. Harris, K. R. Hersey, K. K. Huebner, P. E. Matthews, and T. P. Thomas. 2017. Status and trends of moose populations and hunting opportunity in the western United States. *Alces* 53:99–112.
- NCDC. 2020. Climate data online: dataset directory. 2020.
- Oates, B. A., K. L. Monteith, J. R. Goheen, J. A. Merkle, G. L. Fralick, and M. J. Kauffman. 2021. Detecting resource limitation in a large herbivore population is enhanced with measures of nutritional condition. *Frontiers in Ecology and Evolution* 8:533.
- Owen-Smith, N., and D. Mason. 2005. Comparative changes in adult vs. juvenile survival affecting population trends of African ungulates. *Journal of Animal Ecology* 74:762–773.
- Paterson, T. J., K. Proffitt, J. Rotella, and R. Garrott. 2019. An improved understanding of ungulate population dynamics using count data: Insights from western Montana. *PLoS ONE* 14:1–16.
- Pfister, C. A. 1998. Patterns of variance in stage-structured populations: Evolutionary predictions and ecological implications. *Proceedings of the National Academy of Sciences of the United States of America* 95:213–218.

- Plummer, M. 2003. DSC 2003 Working Papers JAGS: A program for analysis of Bayesian graphical models using Gibbs sampling.
- Proffitt, K. M., M. Hebblewhite, W. Peters, N. Hupp, and J. Shamhart. 2016. Linking landscape-scale differences in forage to ungulate nutritional ecology. *Ecological Applications* 26:2156–2174.
- Raithel, J. D., M. J. Kauffman, and D. H. Pletscher. 2007. Impact of spatial and temporal variation in calf survival on the growth of elk populations. *Journal of Wildlife Management* 71:795–803.
- Ruprecht, J. S., K. R. Hersey, K. Hafen, K. L. Monteith, N. J. Decesare, M. J. Kauffman, and D. R. Macnulty. 2016. Reproduction in moose at their southern range limit. *Journal of Mammalogy* 97:1355–1365.
- Samuel, W. 2007. Factors affecting epizootics of winter ticks and mortality of moose. *Alces* 43:39–48.
- Schrempp, T. V., J. L. Rachlow, T. R. Johnson, L. A. Shipley, R. A. Long, J. L. Aycrigg, and M. A. Hurley. 2019. Linking forest management to moose population trends: The role of the nutritional landscape. *PLoS ONE* 14:1–22.
- Severud, W. J., T. R. Obermoller, G. D. Delgiudice, and J. R. Fieberg. 2019. Survival and cause-specific mortality of moose calves in northeastern Minnesota. *Journal of Wildlife Management* 83:1131–1142.
- Sikes, R. S., and the A. C. and U. C. of the A. S. of Mammalogists. 2016. 2016 Guidelines of the American Society of Mammalogists for the use of wild mammals in research and education. *Journal of Mammalogy* 97:663–688.
- Vartanian, J. M. ., 2012. Habitat Condition and the Nutritional Quality of Seasonal Forage and Diets: Demographic Implications for a Declining Moose Population in Northwest Wyoming.
- Visscher, D. R., and E. H. Merrill. 2009. Temporal dynamics of forage succession for elk at two scales: Implications of forest management. *Forest Ecology and Management* 27:96–106.
- Wattles, D. W., and S. DeStefano. 2011. Status and management of moose in the northeastern United States. *Alces* 47:53–68.

- Weber, N., N. Bouwes, M. M. Pollock, C. Volk, J. M. Wheaton, G. Wathen, J. Wirtz, and C. E. Jordan. 2017. Alteration of stream temperature by natural and artificial beaver dams. *PLOS one* 12.
- Wisdom, M. J., L. S. Mills, and D. F. Doak. 2000. Life stage simulation analysis: Estimating vital-rate effects on population growth for conservation. *Ecology* 81:628–641

Tables

Table 1.1. Numbers of adult female moose (>1 year of age) and calves (9-10 months of age) fitted with GPS collars across 5 regions in Idaho, USA, 2020-2022.

Region	Adults	Calves
Selkirk	28	4
Clearwater	49	3
Lost River	8	0
Bannock	51	5
Island Park	12	5
Total	148	17

Table 1.2. Criteria used to specify models of mortality and reproduction for moose in Idaho, USA, during 2020-2022.

Parameter	Prior Distribution	Number of Iterations	Burn-in	Adaptive phase
Adult Mortality	$\mu \sim \text{Normal}(-0.3, 3)$ T(, -4)	200,000	10,000	2,000
Neonate Calf Mortality	$\mu \sim \text{Normal}(-0.3, 3)$ T(, -3.3)	1,000,000	10,000	5,000
Winter Calf Mortality	$\mu \sim \text{Normal}(-0.3, 3)$ T(, -1.9)	800,000	10,000	2,000
Parturition	$\mu \sim \text{Normal}(-0.3, 1.9)$ T(, -1.4)	200,000	10,000	5,000
Twinning	$\mu \sim \text{Normal}(0, 1.7)$	200,000	10,000	5,000

Table 1.3. Proportional contribution of demographic parameters (elasticity) to proportional changes in population growth of moose in Idaho, USA, 2020-2022.

Rate	Mean	10% quantile	90% quantile
Adult female survival	0.830	0.797	0.865
Yearling survival	0.085	0.067	0.101
Summer calf survival	0.085	0.067	0.101
Winter calf survival	0.085	0.067	0.101
Parturition	0.085	0.067	0.101
Twinning	0.011	0.007	0.016

Table 1.4. Sample sizes used to estimate adult female mortality and reproduction of moose within 5 regions in Idaho, USA, 2020-2022.

Region	Study Year	Adult Mortality	Adult Reproduction	Births Observed	Sets of Twins
Selkirk					
	2019	17	-	-	-
	2020	25	13	7	1
	2021	23	22	13	1
	2022	10	10	7	2
Clearwater					
	2019	38	-	-	-
	2020	48	37	24	4
	2021	37	36	29	5
	2022	16	15	14	6
Lost River					
	2019	8	-	-	-
	2020	8	8	8	0
	2021	3	3	2	0
	2022	1	1	1	0
Bannock					
	2019	31	-	-	-
	2020	49	27	14	2
	2021	31	31	17	2
	2022	18	18	13	3
Island Park					
	2019	8	-	-	-
	2020	10	6	4	0
	2021	6	5	4	0
	2022	3	3	3	0
Total		390	235	160	26

Table 1.5. Mean demographic rates reported for moose populations across the southern extent of their range in North America, 1992-2022.

Source	Location	Year(s)	Adult Survival	Summer Calf Survival	Winter Calf Survival	Adult Pregnancy	Twinning
This Study	ID	2020-2022	0.92	0.69	0.53	0.89	0.14
Lenarz et al. 2010	MN	2010	0.79				
Boer et al. 1992	*NA	1992				0.84	0.33
Debow 2020	VT	2017-2019	0.90,0.84,0.86	0.65	0.60,0.50,0.37	0.67	
Ellingwood et al. 2020	NH	2002-2005	0.87	0.76	0.34	0.75	
Ellingwood et al. 2020	NH	2014-2018	0.8	0.76	0.69	0.78	
Harris et al. 2021	WA	2013-2018	0.8			0.7, 0.93	
Ruprecht et al. 2016	UT	2013-2015				0.74	0.03
Severud et al. 2019	MN	2013-2016		0.58-0.34**			
Musante et al. 2010	NH	2002-2005	0.74,0.87,0.91	0.71	0.67		0.11
Jones et al. 2017	NH/ME	2014-2016		0.77,0.94		0.78,0.88	
Jones et al. 2019	NH/ME	2014-2016			0.30		
Oates 2011	WY	2005-2010	0.84	0.89	0.74***	0.69	0.04
Becker 2008	WY	2004-2006	0.83	0.62		0.92	0.07
Kufeld 1996	CO	1992-1995	0.96				
Murray et al. 2006	MN	1995-2000	0.79				

*Rates estimated throughout North America

**Survival at 30 days – 120 days

***Survival only monitored through February

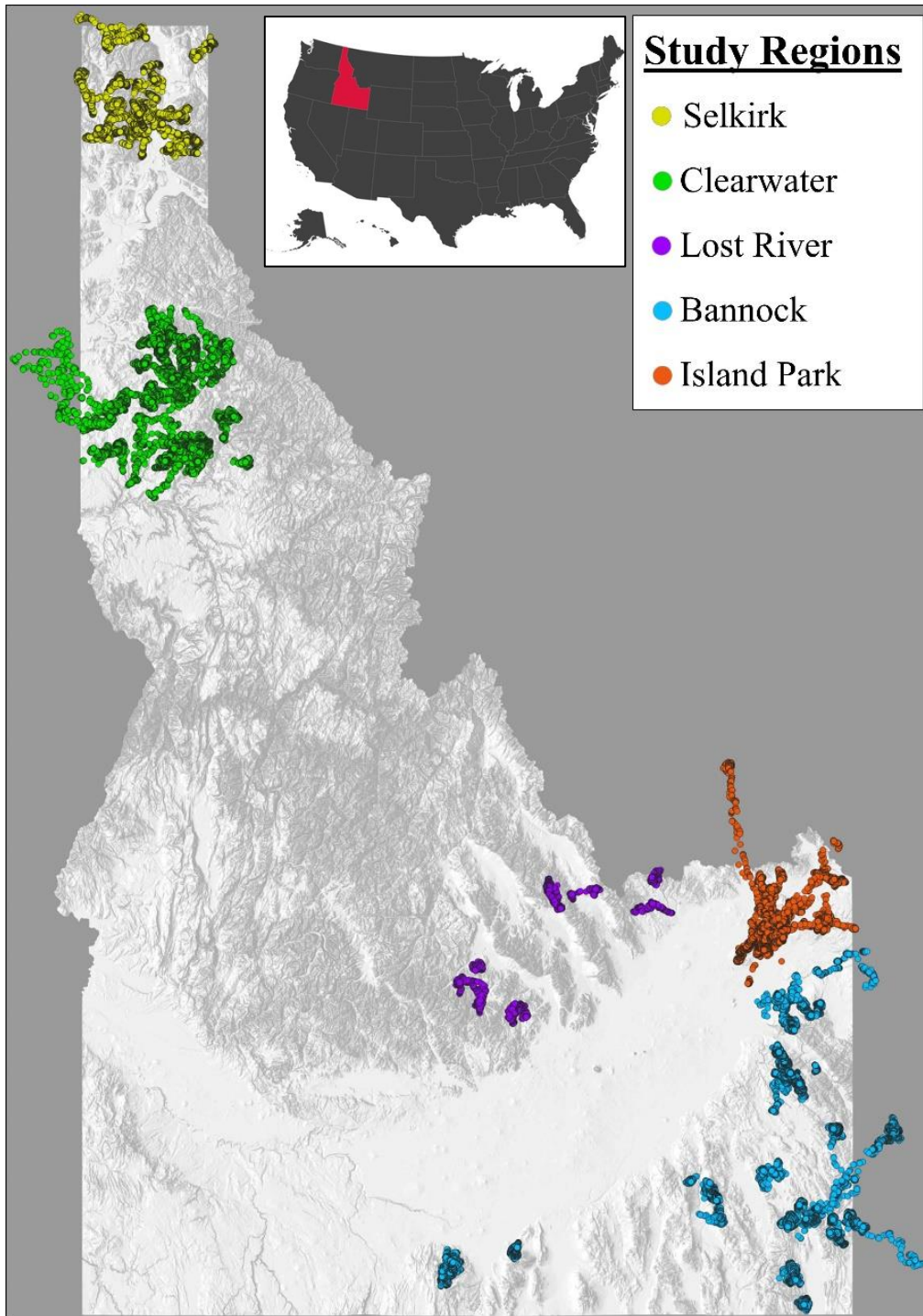
Figures

Figure 1.1. Study regions in Idaho, USA. Circles represent all GPS locations from collared adult female moose during 2020-2023.

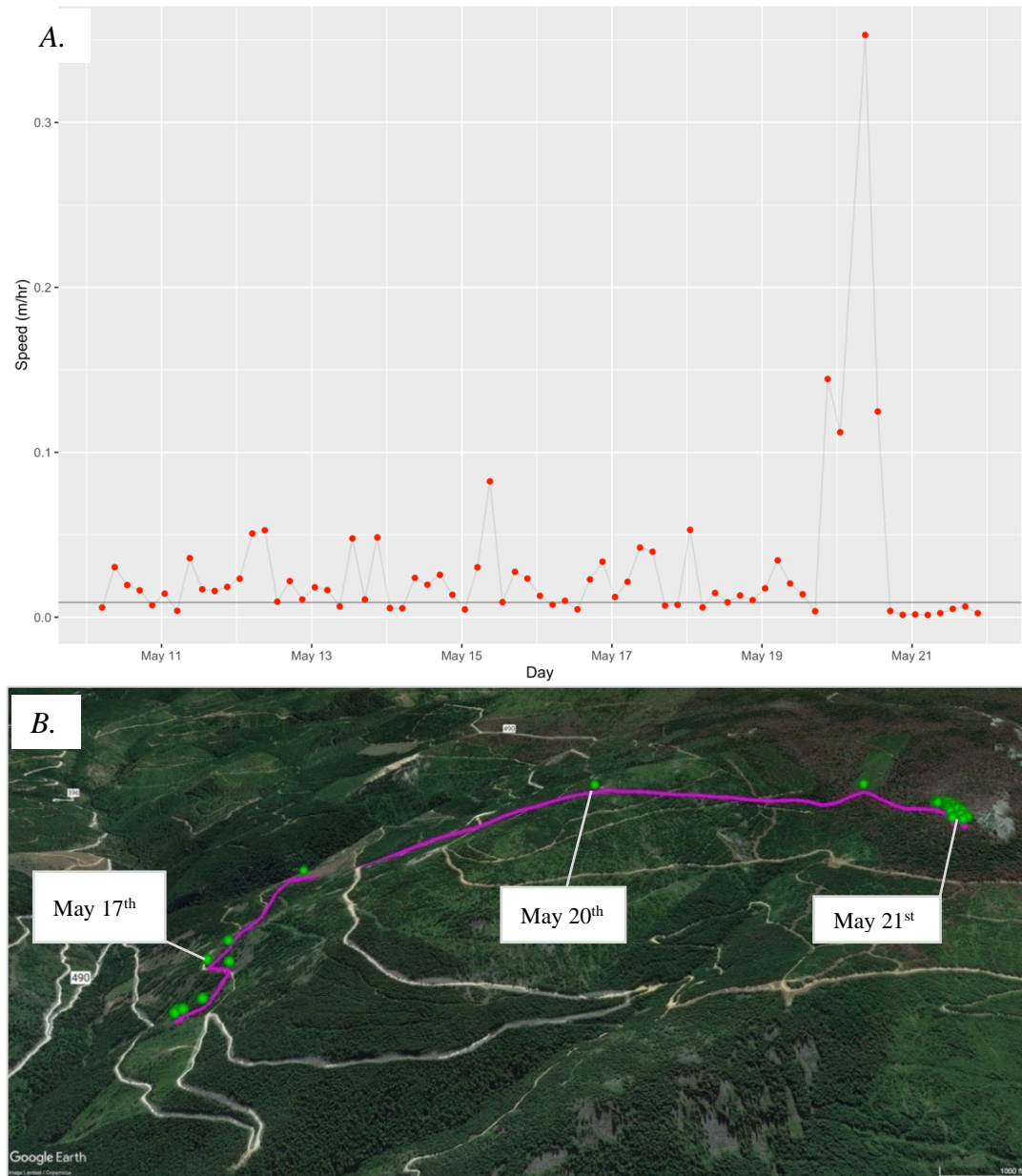


Figure 1.2. Example of a parturition movement from a GPS collared female moose. A) Speed of movement (m/hr) estimated from the distance between GPS locations recorded at 4-hr intervals across 6 days in May. A birth event signified by the sharp increase in speed (~May 20th) followed by a substantial decrease in movements (~May 21st). B) The same birth movement sequence illustrated across the landscape with lines connecting consecutive GPS locations.

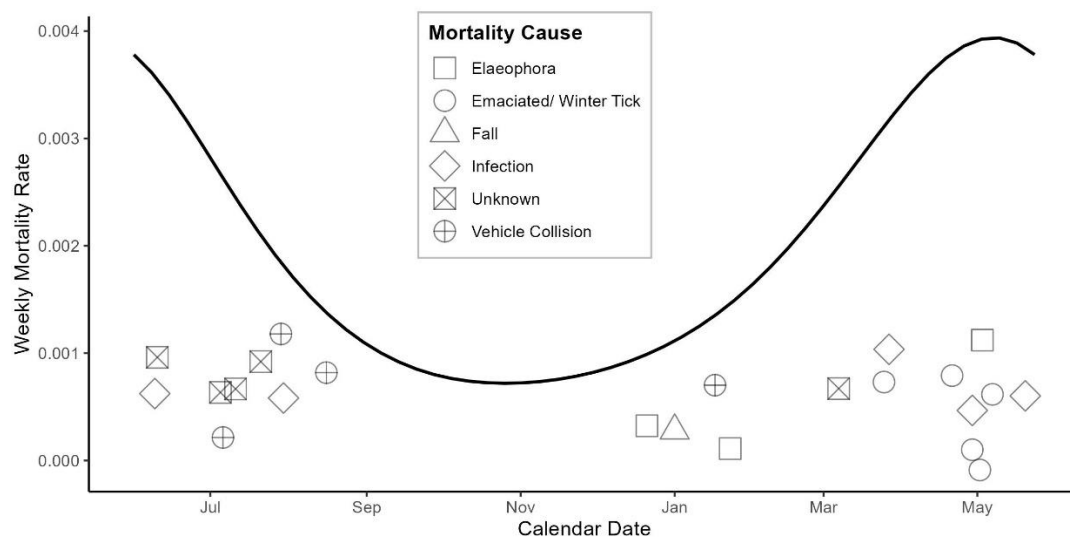


Figure 1.3. Weekly mortality rates of adult female moose (curved line), relative to calendar date in Idaho, USA, 2020-2023. Symbols represent proximate causes of mortality.

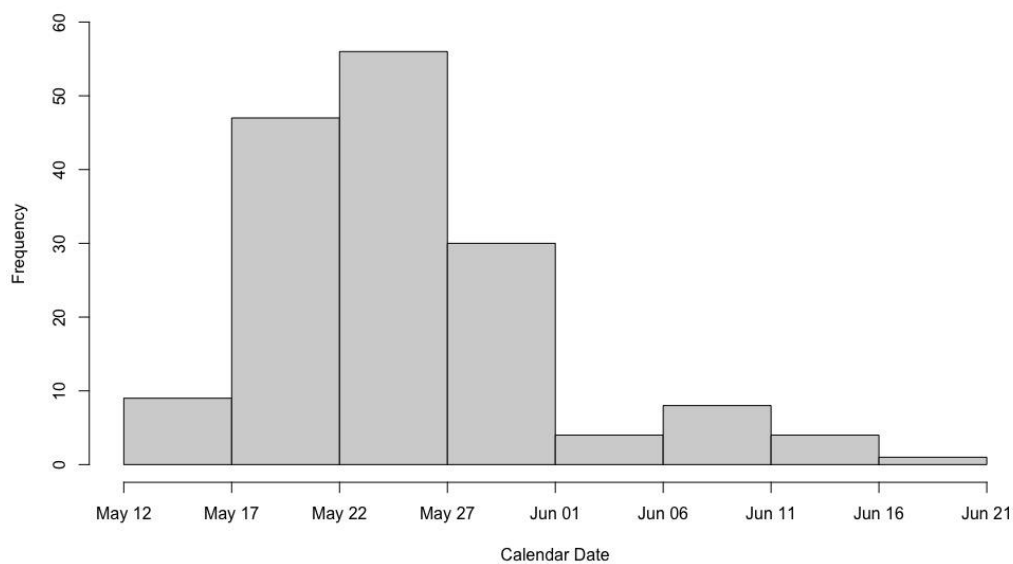


Figure 1.4. Histogram of dates of calving by adult female moose collared in Idaho, USA, 2020-2022.

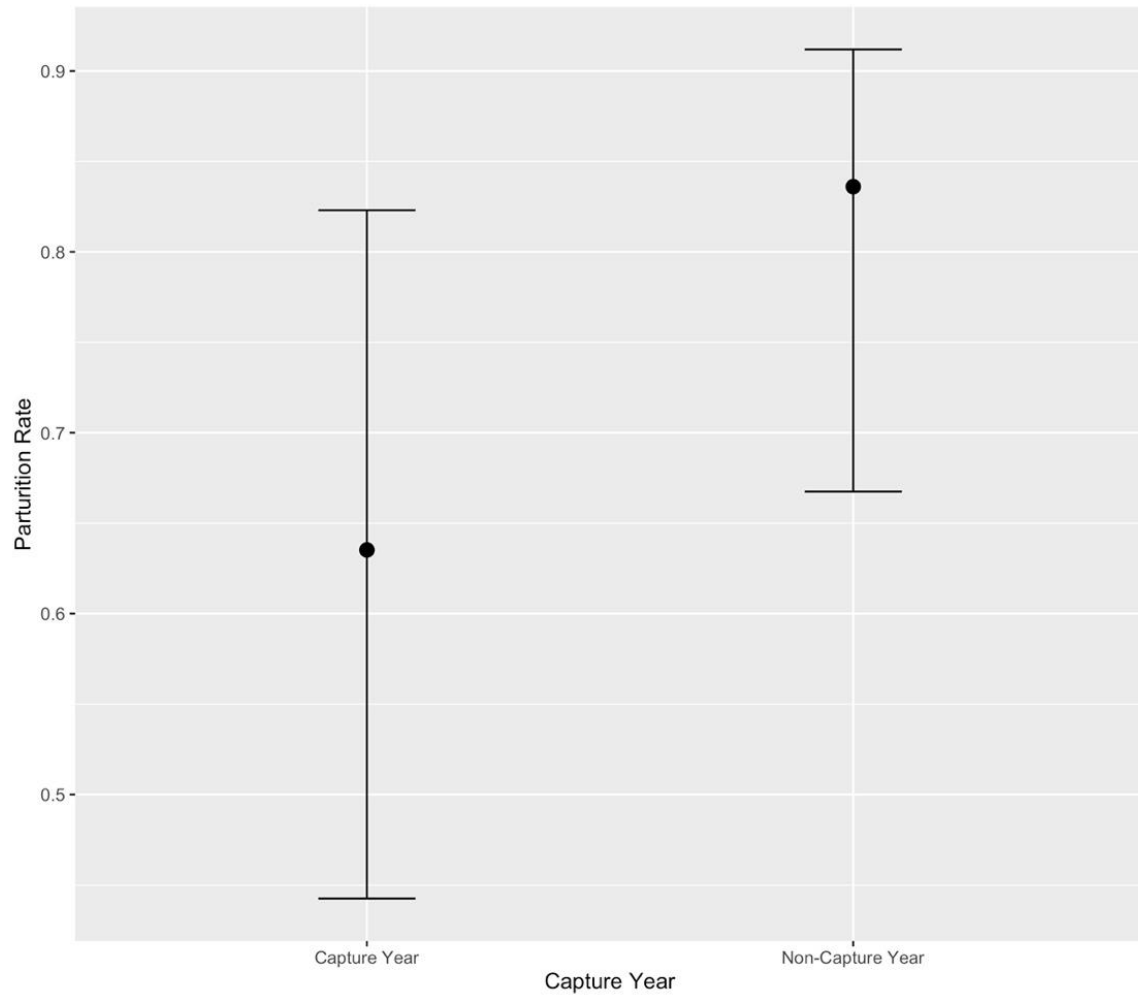


Figure 1.5. Mean parturition rate (\pm 95% credible interval) for adult female moose captured or not within 6 months prior to the parturition window (~15 May - 15 June). Parturition was modeled separately for individuals in capture year and non-capture year.

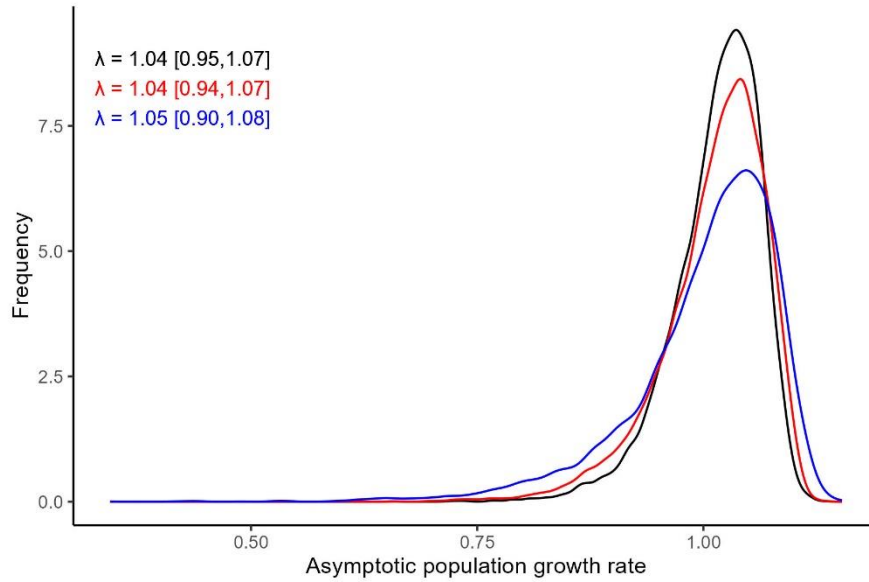


Figure 1.6. Frequency plots of modeled population growth rates for moose in Idaho, USA, based on three variance models: spatial (black), temporal (red), and spatiotemporal (blue) models. Data represent statewide population growth based on demographic rates estimated in 5 regions across 3 years. Also, within each panel, the mode, 10%, and 90% quantiles, are specified for each of the three variance models as follows: $\lambda = \text{mode} [10\% \text{ quantile}, 90\% \text{ quantile}]$.

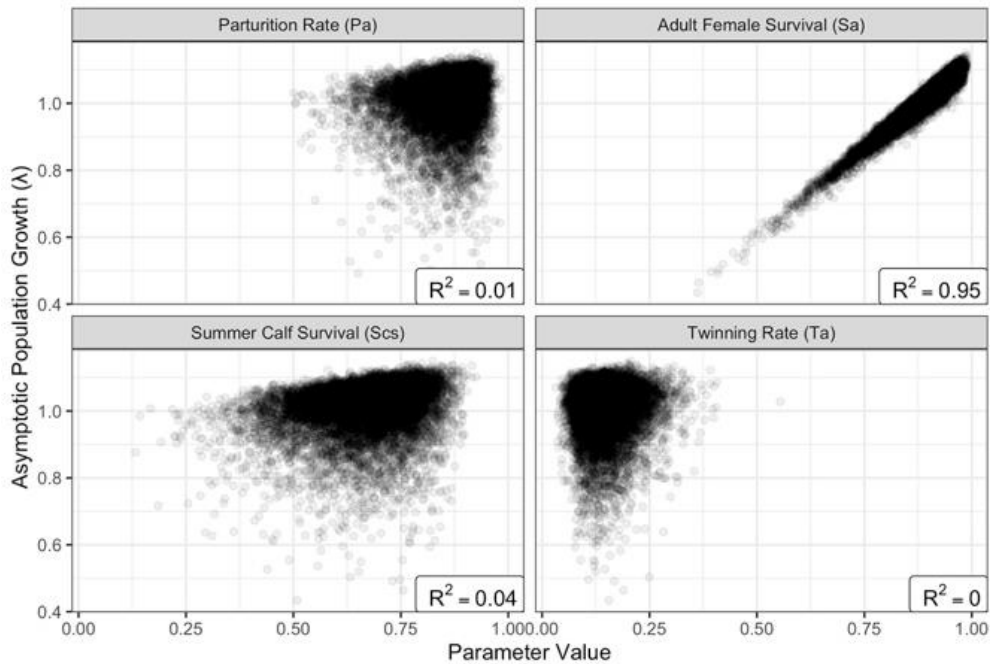


Figure 1.7. Results of Life Stage Simulation Analysis (LSA) for moose populations in Idaho, USA. Plot is subset into four panels, corresponding to the four demographic rates estimated during the study (parturition rate, adult female survival, twinning rate, summer calf survival). Within each panel, black dots represent the relationship between the parameter value and the corresponding population growth rate. Also, within each panel is the R^2 value (LSA value) for each demographic rate.

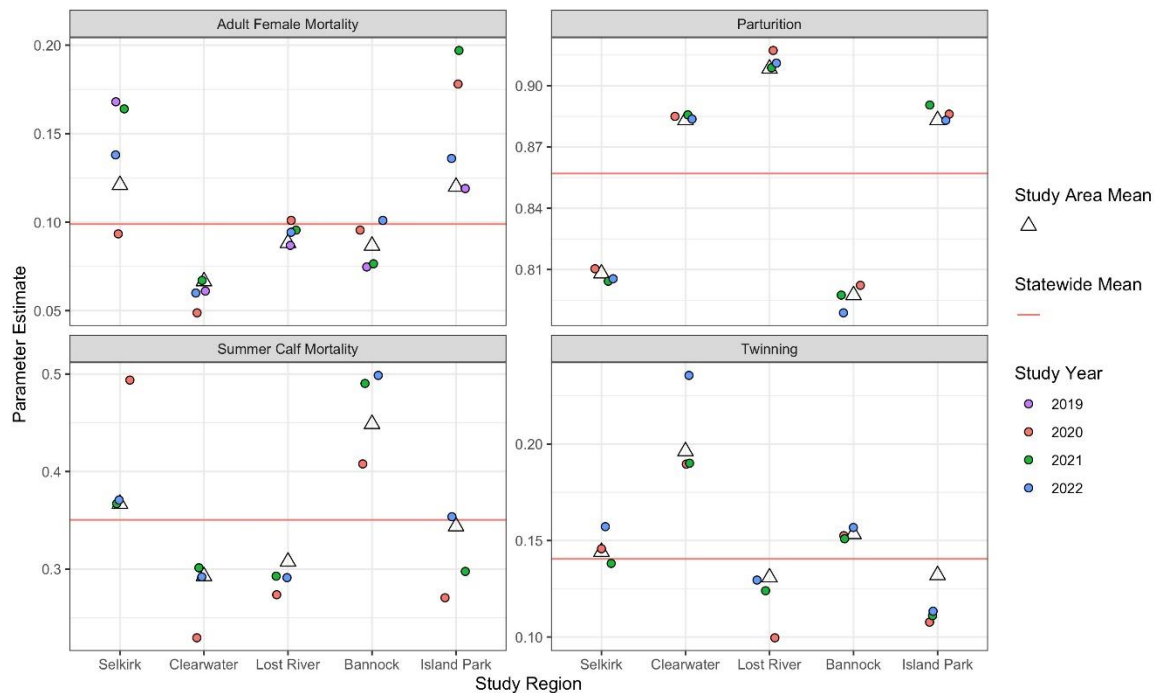


Figure 1.8. Estimated demographic rates by region and year for moose in Idaho during 2020-2022.

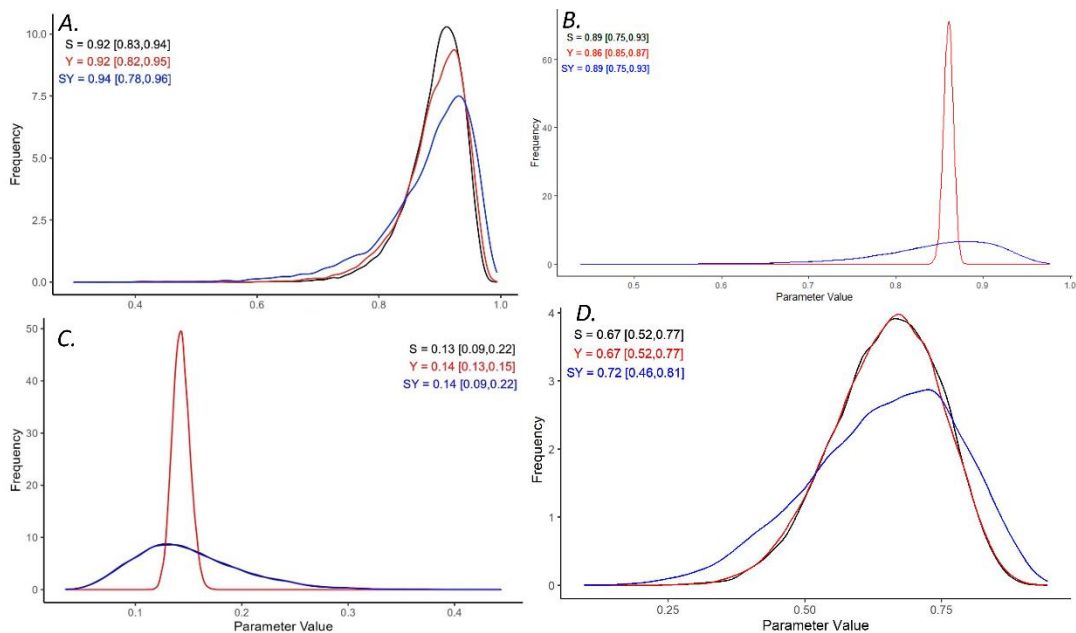


Figure 1.9. Frequency plots of demographic rates for moose in Idaho, 2020-2022, by variance model. Demographic rates include annual adult female survival (A), parturition rate (B), twinning rate (C), and summer calf survival (D). Within each panel the colored lines represent the distributions for each of the 3 variance models: spatial (black), annual (red), and spatiotemporal (blue) models. Also, within each panel, the mode, 10%, and 90% quantiles, are specified for each of the three variance models: $model = mode [10\% \text{ quantile}, 90\% \text{ quantile}]$.

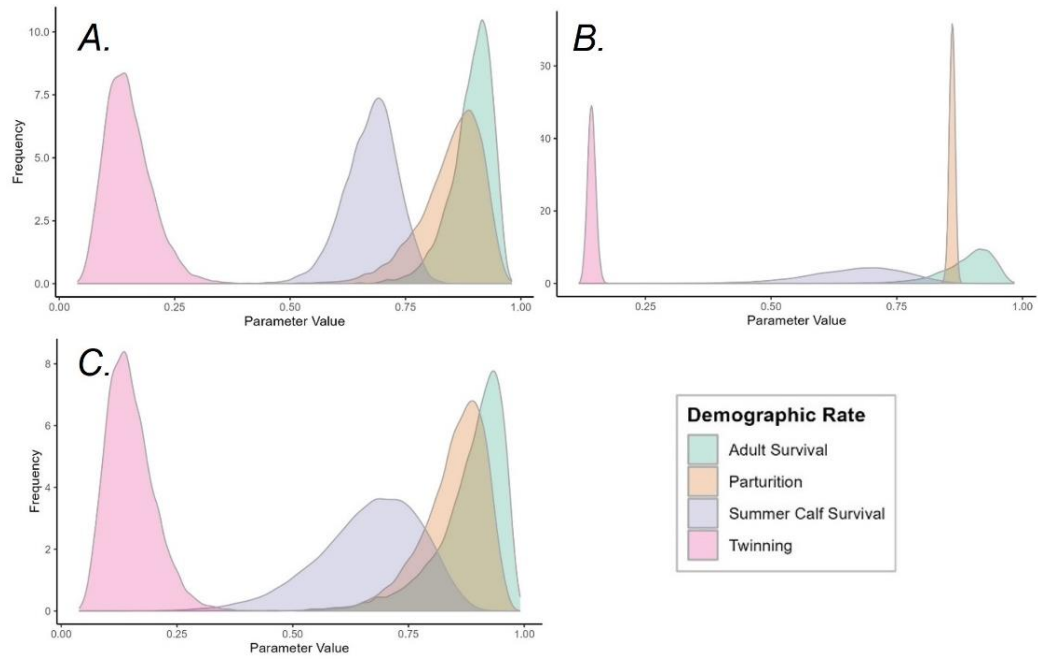


Figure 1.10. Frequency plots of demographic rates for moose in Idaho, 2020-2022, within each variance model: spatial (A), temporal (B), and spatiotemporal (C).



Figure 1.11. Birth sites from collared female moose in Idaho, USA. Photographs show a GPS collared adult female with a newborn calf (A), expelled placenta within a birth site, (B) and typical birth site with matted down vegetation and soil with amniotic fluid (C).

Appendix

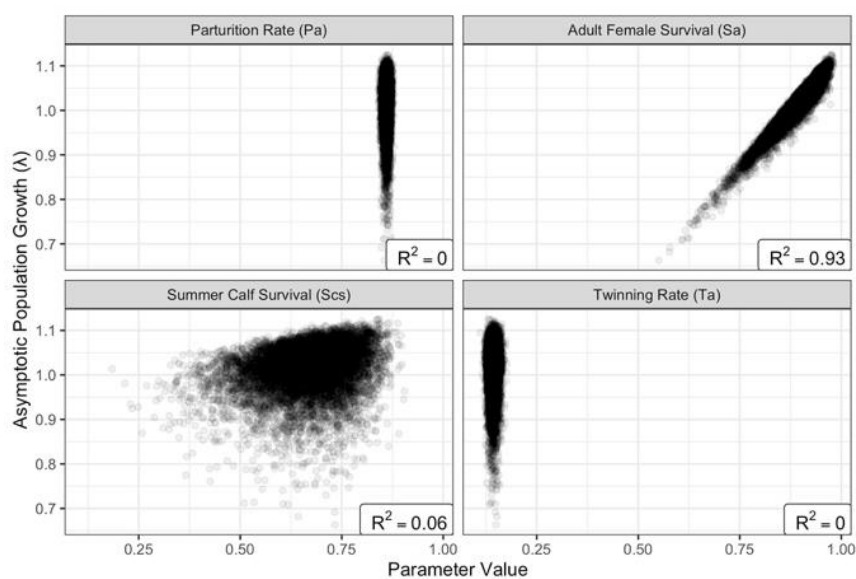


Figure 1.12. Results of Life Stage Simulation Analysis (LSA) from the temporal model. Plot is subset into four panels, corresponding to the four demographic rates estimated during the study (parturition rate, adult female survival, twinning rate, summer calf survival). Within each panel, black dots represent the relationship between the parameter value and the corresponding population growth rate. Also, within each panel is the R^2 value (LSA value) for each demographic rate.

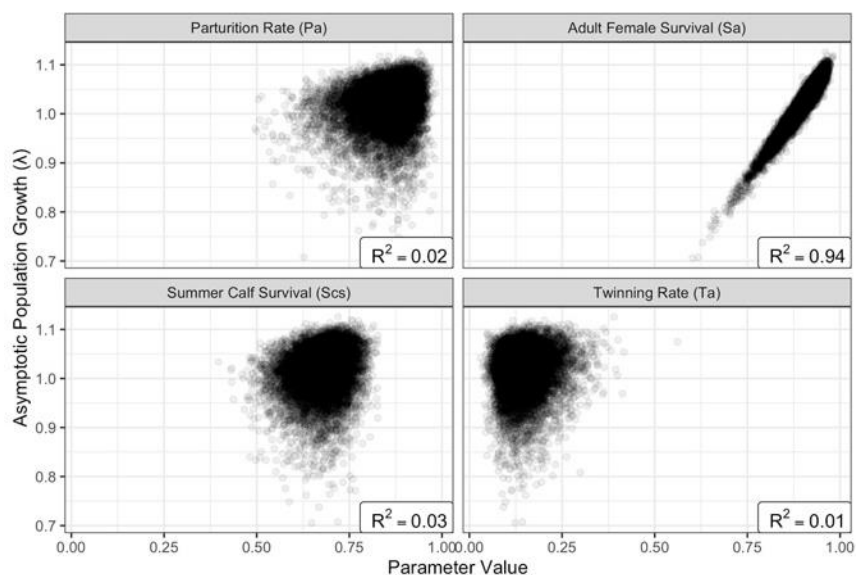


Figure 1.13. Results of Life Stage Simulation Analysis (LSA) from the spatial model. Plot is subset into four panels, corresponding to the four demographic rates estimated during the study (parturition rate, adult female survival, twinning rate, summer calf survival). Within each panel, black dots represent the relationship between the parameter value and the corresponding population growth rate. Also, within each panel is the R^2 value (LSA value) for each demographic rate.

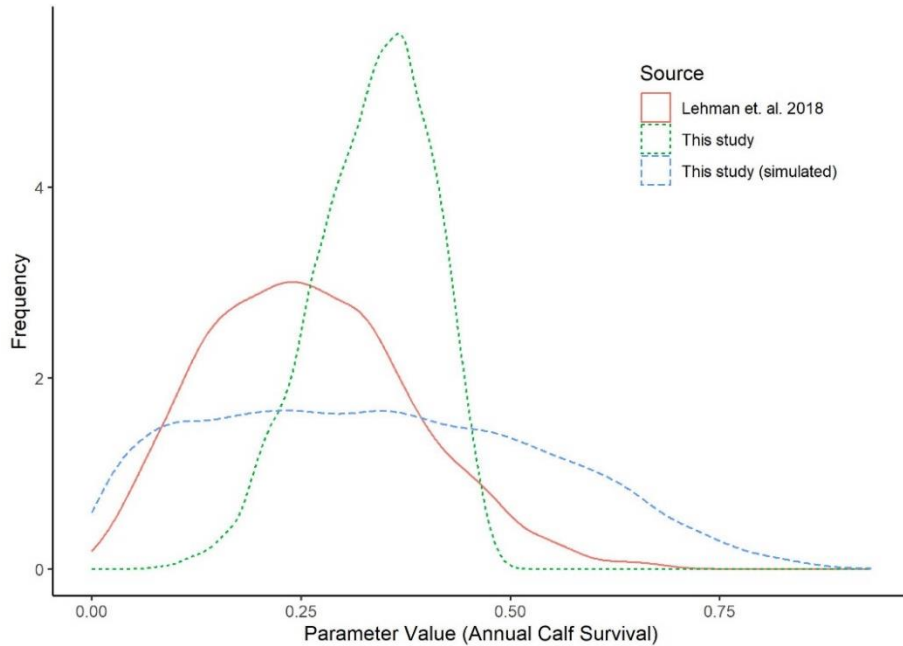


Figure 1.14. Frequency plot of values used for annual calf survival in 3 separate LSAs. The red solid line represents values used in Lehman et al (2018), the green dotted line represents values used in the primary LSA for this study, and the blue dashed line represents values used in the additional LSA for this study and were simulated based on an unrealistically high amount of variation in overwinter calf survival.

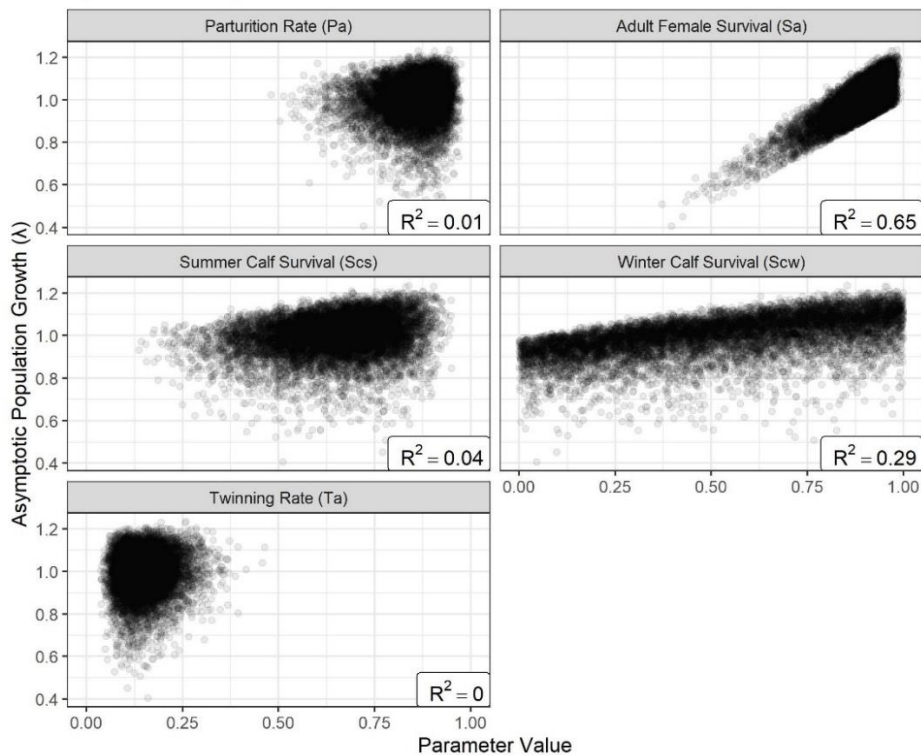


Figure 1.15. Life Stage Simulation Analysis (LSA) results for moose populations in Idaho, USA. Plot is subset into five panels, corresponding to the five demographic rates estimated during the study (parturition rate, adult female survival, twinning rate, summer calf survival, and winter calf survival). Within each panel, black dots represent the relationship between the parameter value and the corresponding population growth rate. Also, within each panel is the R^2 value (LSA value) for each demographic rate. Winter calf survival was simulated to represent an unrealistically high amount of variation for this parameter.

Chapter 2: Elevated Winter Tick Burdens: Potential Cost of Seasonal Site Fidelity by Moose.

Introduction

For many temperate ungulates, variation in seasonal availability of resources results in differential space use throughout the annual cycle. Seasonal habitat selection often results in use of summer ranges that provide high quality and/or abundant forage and winter ranges that reduce energy expenditure as a consequence of less severe temperatures and relatively shallower snow depths (Boyce 1991, Berg et al. 2019, Laforge et al. 2020, Kauffman et al. 2021). Consequently, individuals often exhibit site fidelity to seasonal ranges and migratory strategies that benefit survival and reproduction (e.g., Wiseman et al. 2006, Fullman et al. 2021, Garfelt-Paulsen et al. 2021, Merkle et al. 2022). However, in the face of climate change and increased anthropogenic disturbance, this once adaptive pattern may have negative consequences when habitat quality is impaired (Knick and Rotenberry 2000, Robertson and Hutto 2006, Merkle et al. 2022). Additionally, parasites also may be adapting to target hosts using the same sites and resources in successive years (Teitelbaum et al. 2018). This may be especially important for pathogens and parasites with shorter generation times than long-lived ungulate species, allowing for quicker adaptations to climatic or environmental changes (Chenery et al. 2023).

Winter ticks (*Dermacentor albipictus*) are a single-host parasite that can impose severe metabolic consequences on their hosts. Larval ticks search for hosts during the autumn through an act called ‘questing’, during which tens or hundreds of individual ticks ascend vegetation and aggregate in clumps, waiting for a host to pass by (Lankester and Samuel 2007). After being picked up by a host, winter ticks molt through multiple stages (larvae,

nymph, adult) and mate on the same host after which gravid females detach in early spring to lay their eggs on the ground (Drew 1984, Lankester and Samuel 2007). While on-host, individual ticks take multiple blood meals, with peak feeding occurring as adults and just before detachment in early spring (Samuel and Welch 1991). Throughout all life stages, winter ticks are relatively immobile. Therefore, locations where gravid adult females are dropped from their host in the spring are where larval ticks will be questing in the fall.

The effects of winter tick parasitism are more pronounced in moose compared with other ungulates sharing similar ranges. Blood loss from ticks alone can induce anemia and increase energy expenditure (due to blood replacement), and ultimately decrease survival of moose (Musante et al. 2007). Moose with high tick burdens also expend more energy grooming (i.e., removing ticks through scratching, rubbing, or biting) resulting in hair loss and increased rates of weight loss (Glines and Samuel 1989, Samuel 2004). Furthermore, moose are capital breeders that rely heavily on endogenous fat reserves acquired during the growing season for survival and gestation through late winter (Ruprecht et al. 2016) and loss of blood and fat reserves as a consequence of winter tick infestation compounds energy loss during a nutritionally stressful time (Renecker and Hudson 1989). Research suggests that moose, compared to other ungulate hosts, sustain higher levels of tick infestation throughout the winter, potentially due to their relatively poor ability to groom and behavioral response to irritation from tick infestation (Mooring and Samuel 1998, Welch et al. 2011). If this hypothesis is true, then moose should be the primary hosts propagating winter tick populations across the landscape (Mooring and Samuel 1998, Welch et al. 2011).

In recent decades, declines in populations of moose have been documented across the southern extent of their range in North America (Wattles and DeStefano 2011, DeCesare et

al. 2012, Mech and Fieberg 2014, Nadeau et al. 2017). Although multiple factors likely interact to influence populations, disease-causing parasites including winter ticks (Samuel 2004), carotid artery worms (*Elaeophora schneideri*; Henningsen et al. 2012), and meningeal worms (*Parelaphostrongylus tenuis*; Nagy 2004), can contribute to population declines. In particular, the winter tick appears to be expanding its range northward, threatening the stronghold of moose in North America (Chenery et al. 2023). This concern is well warranted with recent research suggesting that ticks can have population-level effects on moose in the northeastern USA (Musante et al. 2010, Jones et al. 2019). During epizootic years, winter tick infestation substantially decreased annual calf recruitment, and although survival of adult females is rarely affected by such epizootics, reproduction and survival of young can be reduced during the following year (Jones et al. 2017, Pekins 2020).

Winter tick distribution across the landscape can be defined by a combination of three factors: the density of hosts, suitability of environmental conditions for off-host survival and reproduction, and spatial overlap between host ranges during the period when gravid females are dropping off in the spring and when larvae are questing for hosts in the fall. Because adult female ticks are relatively immobile and typically lay their eggs within a meter from where they drop off their host (Drew and Samuel 1986), locations where gravid female ticks are dropped in the spring is where larval ticks will be picked up by new hosts in the fall. Therefore, the risk of picking up larval ticks in the fall should be related to the distribution of resources used by hosts during the spring drop-off period (Healy et al. 2018, Blouin et al. 2021).

The goal of this study was to relate the relative winter tick burden on moose to resource use during the spring drop-off and fall questing periods. We first created resource

selection functions (RSFs) for moose within 6 study regions in Idaho, USA, during the spring drop-off period for winter ticks (15 March – 15 May). We then used the RSFs to predict the relative probability of use by moose during the spring drop-off period across each region, which we interpreted as the “tick risk landscape”. Finally, we overlaid locations of moose during the fall questing period onto the tick risk landscape. We hypothesized that time spent by moose in risky areas during the fall questing period would increase exposure to winter ticks, and we predicted that individuals that made relatively greater use of risky areas would experience higher tick loads. Findings from this study contribute to understanding the relationship between winter ticks and moose, and could help to identify areas on the landscape as well as habitat conditions that are important for transmission of ticks, thereby providing a foundation for developing management strategies to mitigate the influence of winter ticks on moose populations.

Methods

Study Regions – This study was conducted within 5 regions in Idaho, USA, selected to represent most of the range and hunting opportunity for moose within the State (Fig. 2.1). The study regions encompass broad ecological variation extending from the northern to the southern borders of the State, and they represent three major ecoregions that are characterized by various habitat types, predator complexes, and densities of moose and other ungulates.

Two of the study regions (Selkirk and Clearwater) are located within the Northern Rockies Ecoregion. The Selkirk region is characterized by high topographic relief with elevations ranging from 450 to 2,300 m. This area is dominated by mixed coniferous forest with common species including grand fir (*Abies grandis*), western red cedar (*Thuja plicata*), western hemlock (*Tsuga heterophylla*), larch (*Larix occidentalis*), and white pine (*Pinus*

strobis). The area experiences high annual precipitation ranging from 56 to 140 cm per year with mean monthly temperatures ranging from -9 to 30 °C (NCDC 2020). The Clearwater region is characterized by diverse topography ranging from gently sloping hills to steep mountains with elevations of 450-2,000 m, annual precipitation from 61 to 165 cm, and mean monthly temperatures ranging from -7 to 28 °C (NCDC 2020). Dominant tree species include western red cedar, western hemlock, and white pine, with intensive logging occurring across much of the region.

Two study regions (Lost River and the Island Park) are encompassed within the Middle Rockies Ecoregion. Lost River is topographically diverse with low-elevation valley floors dominated by grass and shrubland species and high-elevation alpine and montane environments dominated by western spruce (*Picea sitchensis*), Douglas fir (*Pseudotsuga menziesii*), and lodgepole pine (*Pinus contorta*). Elevations range from 1,158 to 3,859 m, mean annual precipitation ranges from 15 to 112 cm, and mean monthly temperatures range from -17 to 29 °C (NCDC 2020). Within the Island Park region, dominant tree species include Douglas fir and lodgepole pine, interspersed with shrub-steppe habitat dominated by sagebrush (*Artemisia* spp.). Island Park, which is located at relatively high elevations (1,500-2,900 m), receives between 15 and 102 cm of precipitation annually with mean monthly temperatures ranging from -17 to 31 °C (NCDC 2020).

The Bannock-A and Bannock-B study regions are located within the Northern Basin and Range Ecoregion with elevations spanning 900-2,700 m, mean annual precipitation from 20 to 76 cm, and mean monthly temperatures ranging from -13 to 29 °C (NCDC 2020). These regions are dominated by multiple tree species including western spruce, Douglas fir, lodgepole pine, and bigtooth aspen (*Populus grandidentata*).

Animal Capture – We captured adult female moose between January and March of 2020 and 2021. All moose were darted from a helicopter and fitted with global position system (GPS) collars (G5-2D Iridium, Advanced Telemetry Systems, Isanti, MN, USA) that were programmed to drop off ~2 years after deployment. All collars were programmed to record a location every 4 hours, transmit locations to a satellite twice per day, and send an email notification if stationary for > 6 hours, signaling a mortality event. For all captured moose, we estimated relative tick load by counting winter ticks on the hindquarters of immobilized individuals. During 2020, we counted the total number of ticks observed along a 10-cm transect centered on the hind quarter of the moose (Samuel 2004). We parted the hair with a wide-toothed comb and counted winter ticks present, most of which were embedded in the skin. During 2021, the total number of ticks was enumerated within a 10x10 cm patch, centered in the same location, by using a comb to make successive parts in the hair across the patch to survey the skin surface. Transects and patch counts are related, however, not directly comparable (Sine et al. 2009). Therefore, we categorized relative tick burdens across individuals within each year. All capture and animal handling procedures were approved by the University of Idaho Institutional Animal Care and Use Committee (IACUC protocol 2020-17) and followed guidelines for use of wild mammals in research (Sikes et al. 2016).

Habitat selection – We modeled selection of habitats by moose during the spring tick drop-off period within 6 regions across the State. We considered a total of 10 habitat parameters (Table 2.1), including 5 continuous variables derived from the 2019 United States Geological Survey (USGS) digital elevation model (DEM) and 5 categorical variables derived from the 2019 National Land Cover Database (NLCD, Jin et al. 2019). Topographic covariates included elevation, slope, topographic position index (TPI), sine of aspect, and

cosine of aspect. We also included a squared term for slope, TPI, and elevation to allow for non-linear relationships associated with these three variables. Vegetation categories included evergreen forest, deciduous forest, mixed forest, shrub, and herbaceous (Table 2.1).

We used a 2-scale (broad and local) use versus availability framework to model habitat selection, which evaluated the characteristics of the general area selected by moose as well as fine-scale characteristics within general use areas. Used locations for both scales were defined as GPS locations from collared adult females during 15 March–15 May. This timeframe was chosen to represent habitats used by moose when gravid female winter ticks are dropping off (Healy et al. 2018, Blouin et al. 2021). We selected one used location within every 80 hours for each moose-year to reduce the total number of locations for computational efficiency. At the broad scale, the extent of availability was quantified as a minimum convex polygon (MCP) that included all moose GPS locations within each region. Available locations were then generated by distributing 3000 points evenly across the entire MCP. Covariate values for both used and available locations were extracted from each of the covariate layers as the mean (or proportion for categorical variables) of cell values for that variable within a 2.6 km circle centered on each location. At the local scale, the extent of availability was quantified as a 2.6 km circle centered on each used location, and available locations were then generated by distributing 300 points evenly throughout this circle. At the local scale, covariate values for used and available locations were extracted from each of the covariate layers as the cell value for that covariate at the location.

We then modeled the probability of use during the spring drop-off period as:

$$\mu_s = \frac{w(X_s, \beta) a_s}{\int_{g \in G} w(X_s, \beta) a_g dg}$$

where μ_s is the probability of selection at position s , X is a vector of environmental variables at position s , and β is a vector of selection coefficients estimated using conditional logistic regression. The denominator scales μ_s from 0 to 1 ensuring it remains a proper utilization distribution, a represents the availability distribution and g represents either the MCP boundary (broad-scale analysis) or the 2.6 km circle around each location (local-scale analysis).

We created a set of region-specific models at both scales to evaluate resource selection. Within each region, we excluded covariates that represented <3% of used locations, and we did not use those that were correlated ($r > 0.60$) in the same region-scale model sets. The baseline model for each region and scale included only vegetation cover covariates, and other models included combinations of vegetation and topographic parameters. Elevation was withheld from all local-scale models because selection for elevation was assumed to occur primarily at the broad scale. Similarly, TPI was withheld from all broad-scale models because selection for TPI was assumed to occur primarily at the local scale. After fitting scale-specific models for each region, we used Akaike Information Criteria (AIC) to evaluate weight of evidence for models and identify the models that were best supported by the data.

Within each region, the top models from both the broad and local-scale analyses were used to predict spring moose habitat across each region. Broad-scale resource use was predicted as:

$$P_b(A_s) = \frac{w(X(A_s), \beta_s)}{\max [w(X(A_s), \beta_s)]}$$

where (β_s) is the vector of parameter estimates from the top broad scale model, $X(A_s)$ is a vector of mean values of each covariate within the 2.6 km circle, and the denominator scales (P_b) from 0 to 1 ensuring it remains a proper utilization distribution. Local-scale resource use was the predicted as:

$$P_l(s) = \frac{w(X_s, \beta_s)}{\max [w(X_s, \beta_s)]}$$

where (β_s) is the vector of parameter estimates from the top local scale model, X_s is a vector of each covariate value position s , and the denominator scales (P_l) from 0 to 1 ensuring it remains a proper utilization distribution. We then calculated the relative probability of selecting a used location conditional on having already selected the broad area as:

$$R_l(s) = \frac{P_l(s)}{\text{mean}[P_l(A_s)]}$$

where $\text{mean}[P_l(A_s)]$ was the mean of $P_l(s)$ within the 2.6-km circle centered on position s . By dividing the value of $P_l(s)$ by this expected value, $R_l(s)$ provides a measure of the relative increase or decrease in the probability that position s would be selected, given that a moose chose to use A_s . We obtained the final prediction, by combining the relative local prediction (R_l) and the broad scale prediction (P_b) as:

$$P(s) = \frac{P_b(A_s) * R_l(s)}{\max [P_b(A_s) * R_l(s)]}$$

the final prediction ($P_{(s)}$) represents the relative probability of use by moose during the spring drop-off period across each region (i.e., the tick risk landscape). Final predictive models were evaluated by constructing and visually inspecting receiver operating characteristic curves (ROC) and estimating the area under the curve (AUC) for each regional model.

Fall Locations – We used GPS locations from collared moose during 15 September–15 November of each calendar year to represent habitat use when moose are likely picking up ticks during the fall questing period. We removed locations that were <4 hours apart and additional outliers identified by visual inspection. We used data from each individual in each year, and only used individual-years that had ≥ 300 locations (mean = 353) in their fall range. Locations were overlaid onto the region-specific tick risk landscape, and the cell value was extracted for each location. Cell values were then averaged within a given year for each individual. Individual-year averages were then averaged again for each individual, resulting in one estimate of exposure to winter ticks during the fall questing period for each individual moose (i.e., “tick risk value”). Tick burden was assessed at the same time GPS collars were deployed, and therefore, we do not have fall location data to estimate use of the tick risk landscape at the time that the individual acquired the questing ticks. However, because individuals tended to be faithful to their fall range within the tick risk landscape across years (App. 2.6), we assumed that the average of tick risk values across years of available data represent relative use of the tick risk landscape during the year in which the tick count was conducted.

Tick-risk analysis – We used ordinal logistic regression models to assess the relationship between potential exposure to ticks during fall and tick burden during late winter. We considered the tick risk value from fall habitat use as the predictor variable and

tick count assessed at the time of capture as the response variable. Because tick counts were conducted differently between capture years, we standardized tick counts among capture years by setting the highest count in each year to a value of 1 and rescaling all counts from 0 to 1. We then developed a relative index of tick burden by binning tick count values into low ($<1/3$ quantile), medium ($\geq 1/3$ quantile to $<2/3$ quantile) and high ($\geq 2/3$ quantile) tick counts for each year. These bins were then used in the ordinal regression models, and we developed a set of candidate models to assess factors influencing the relative tick burden that included unique combinations of region, capture year, and animal ID (random intercept). We ran ordinal regression models using the *clm* and *clmm* functions from the *ordinal* package in program R, used Akaike Information Criteria (AIC) to evaluate support for the models, and assessed goodness of fit using Nagelkerke's pseudo- R^2 (Nagelkerke 1991).

Results

We used 4,388 GPS locations from 136 adult female moose (229 individual-years) for analyses of habitat selection during the spring winter tick drop-off period. Across all regions, the majority of locations were in shrub (49%) and evergreen forest (37%) cover types, however, proportions varied among regions (Tables 2.2). Another 9% of locations were in deciduous forest (5%), herbaceous (2%), and mixed forest (2%) cover types. The remaining 5% of locations were in various cover types (e.g., woody wetland, wetland, developed, crop, water), however, none of the cover types represented $\geq 3\%$ of locations within a region. Therefore, these cover types were not used in analysis, and locations within these habitats were assigned null values.

Both vegetation and topographic characteristics influenced habitat use by female moose during the spring tick drop-off period. At the broad scale, the top ranked models across all regions included evergreen forest, shrub, and all of the topographic covariates used

in the broad-scale analysis (sine of aspect, cosine of aspect, elevation, elevation², slope, and slope²; Table 2.3). In addition, the broad-scale models across most regions also included mixed forest and herbaceous cover types (Table 2.3, Fig. 2.3). At the local scale, the top ranked models across all regions contained the categorical variable for vegetation type, sine of aspect, cosine of aspect, slope, and slope² (Table 2.4). Also at the local scale, all regional models except the Selkirk region contained TPI and TPI² (Table 2.4, Fig. 2.4). For a few regional and local-scale model sets, competing models were identified (Tables 2.3-2.4), however, the top models were well supported within each model set (model weights = 0.82 – 1.0 for broad scale and 0.68 – 1.0 for the local scale). Within each region we combined the top model from each scale to predict the relative probability of use by moose during the spring drop-off period. The final models for predicting habitat selection (Fig. 2.2-2.3) within each region performed well in terms of specificity (probability of predicting habitat, conditioned on moose being present at a location) and sensitivity (probability of not predicting habitat conditioned on moose being absent at a location) (AUC=; 0.70-0.92; Fig. 2.4).

Model results suggested that exposure to the tick risk landscape was positively associated with relative tick burden. We modeled the relationship between tick burden and the tick risk landscape using 82 individual moose across the 6 study regions. We found support for two models ($\Delta AIC < 4$) in explaining the relationship between tick burden and the tick risk landscape. The best supported model that carried 70% of the cumulative model weight, included tick risk value and study region. The second-best model ($\Delta AIC = 2.63$) only included study region but had much less weight ($\omega_i = 19\%$). The top model indicated that as moose spent more time within the tick risk landscape, the odds of acquiring more ticks

increased (OR= 6.49, 95% CI = 2.5 – 17.0). Predictions from the top model illustrate the probability of acquiring a low, medium, or high tick load relative to use within the tick risk landscape (Fig. 2.5)

Discussion

Our results suggest that individual seasonal site fidelity influenced interactions between winter ticks and moose. Using predictive maps from our spring RSFs to create a tick risk landscape and locations of moose during the fall tick questing period, we demonstrated that the relative burden of winter ticks that a moose experienced can be attributed, in part, to their use of similar resources during both seasons. The probability that a moose would experience a high, medium, or low relative tick load during winter was associated with use of risky habitats; our top model indicated that use of risky landscapes during the fall increased the likelihood of picking up winter ticks. This work highlights an underappreciated cost of site fidelity, specifically transmission of parasites and disease among individuals of the same species. Winter tick infestations are especially costly for moose, and although moose are not considered social, their seasonal site fidelity likely contributes to perpetuating the life cycle of the winter tick and intensifying their impacts on moose.

Habitats varied widely among our study regions, yet similar relationships between tick burden and the tick risk landscape were observed across regions. Regardless of broad environmental variables, moose that showed similar patterns of habitat use between spring and fall acquired more ticks. Other studies have also documented seasonal range fidelity in moose, and it is likely that individuals are keying in on early successional habitats that provide adequate shelter and forage during both the spring and fall months (Healy et al. 2018, Blouin et al. 2021). Furthermore, individual moose tended to use the same areas on the tick risk landscape in successive years, resulting in similar exposure to winter ticks (App.

Fig. 2.8), and likely contributing to variation among individuals in parasite burdens and metabolic consequences.

Our estimate of the tick risk landscape was based only on the distribution of habitats used by moose when gravid females detach from their hosts during spring. Other environmental factors also likely affect tick burdens on moose (Drew and Samuel 1986). For example, survival of ticks during the larval stage, varies due to fluctuations in temperature, humidity, and precipitation (Holmes et al. 2018). These factors also influence the amount of time larval ticks can spend questing during the fall, which is directly related to annual tick infestation levels on moose (Healy et al. 2020). Additionally, habitat types can influence larvae-to-host transmission. Specifically, dense, and heterogeneous vegetation such as brush and shrubs, increases contact and consequently, transmission, between ticks and their hosts (Drew and Samuel 1985*a*). Identifying resource and environmental variables important for larval tick survival and ability to quest is critical for better understanding the winter tick life cycle and subsequent moose infestation levels. Incorporating environmental factors that influence survival of gravid adult female ticks during the spring and early summer, survival of eggs during late summer, and survival and questing by larvae during fall would inform our relatively coarse estimate of the tick risk landscape and more fully represent exposure to ticks experienced by moose during autumn. Nonetheless, our results indicated that resource use by moose during the spring and fall seasons alone can help to predict winter tick burden.

Likewise, our estimate of relative tick burden also was coarse, but demonstrated a positive response to use of risky landscapes by moose. Patch and transect counts on moose have been widely used to index relative tick burdens (Samuel 2004, Sine et al. 2009). Even though the areas sampled are small and the numbers of ticks on moose can be extreme

(>100,000; Samuel 2004), these indices have been evaluated and demonstrated to represent relative total tick burdens (Sine et al. 2009). Additionally, because males typically exhibit greater movements than females during the rut, which coincides with the tick pick-up period, their tick burdens are expected to be higher than females. Our study only examined resource use and overlap by adult females, and investigating movements by males and their influence on transmission of winter ticks is needed to refine estimation of the tick risk landscape.

The relationship between moose and the tick risk landscape demonstrates a complex interaction between host, parasite, and environment. Although winter ticks infest other ungulates (e.g., white tailed deer, *Odocoileus virginianus* (MacHtinger et al. 2021); elk, *Cervus canadensis* (Calvente et al. 2020), and caribou, *Rangifer tarandus* (Welch et al. 1990)), moose appear to serve as a primary host in the northern portions of the continental USA (Welch et al. 2011). This relationship is perhaps a result of higher infestation rates on moose relative to other mammals as well as sympatric seasonal range use by moose, both of which could result in higher transmission rates among moose. Further exploring factors that influence the winter tick-moose relationship could help reveal the underlying evolutionary mechanisms perpetuating the annual life cycle of the winter tick and inform development of strategies for mitigating their increasing impact on moose populations across North America.

For many species, faithfulness to sites, routes or landscapes across seasons, years, and even generations has led to an increase in fitness and higher reproductive output for individuals that exhibit site fidelity (Turner 1989, Bose et al. 2017). However, for some species, climate change and increased anthropogenic disturbances could quickly reverse the effects of these once beneficial behaviors (Forrester et al. 2015, Merkle et al. 2022). Identifying the mechanisms that shaped the evolution of site fidelity can inform our

understanding of why certain individuals exhibit fidelity, and also advance our ability to predict when and how the consequences of continued fidelity might differ in rapidly changing environments.

Management Implications

Winter ticks have been associated with population declines of moose across the southern periphery of their range in North America. High infestation levels of winter ticks can impose severe metabolic costs on moose and reduce survival of juveniles. High tick infestations also result in lower reproductive rates and survival of offspring following epizootic years (Pekins 2020). While numerous strategies to reduce winter tick numbers on the landscape have been proposed, most have not been applied at a large enough scale to yield population-level benefits. Recommended mitigation actions have included prescribed fire (Drew and Samuel 1985*b*), introduction of a fungus known to kill winter ticks (Sullivan et al. 2020), and reduction of moose densities (Ellingwood et al. 2020). Even if these strategies can reduce the number of ticks on the landscape, it is unclear whether they can be effective at reducing tick burdens and the metabolic and demographic consequences of the parasite on moose populations. One challenge of off-host tick reduction efforts is the broad extent of land that needs to be treated. However, applying the concept of the tick risk landscape could help to focus land treatment and reduce the area over which habitat manipulations would be required. Additional research that expands understanding of environmental factors propagating tick populations and promoting transmission among moose is needed to inform comprehensive strategies to reduce the impact of winter ticks on moose populations in North America.

Literature Cited

- Berg, J. E., M. Hebblewhite, C. C. St. Clair, and E. H. Merrill. 2019. Prevalence and mechanisms of partial migration in ungulates. *Frontiers in Ecology and Evolution* 7.
- Blouin, J., J. DeBow, E. Rosenblatt, J. Hines, C. Alexander, K. Gieder, N. Fortin, J. Murdoch, and T. Donovan. 2021. Moose habitat selection and fitness consequences during two critical winter tick life stages in Vermont, United States. *Frontiers in Ecology and Evolution* 9:1–17.
- Bose, S., T. D. Forrester, J. L. Brazeal, B. N. Sacks, D. S. Casady, and H. U. Wittmer. 2017. Implications of fidelity and philopatry for the population structure of female black-tailed deer. *Behavioral Ecology* 28:983–990.
- Boyce, M. S. 1991. Migratory behavior and management of elk (*Cervus elaphus*). *Applied Animal Behaviour Science* 29:239–250.
- Calvente, E., S. Pelletier, J. Banfield, J. Brown, and N. Chinnici. 2020. Prevalence of winter ticks (*Dermacentor albipictus*) in hunter-harvested wild elk (*Cervus canadensis*) from Pennsylvania, USA (2017–2018). *Veterinary Sciences* 2020, Vol. 7, Page 177 7:177.
- Chenery, E. S., N. J. Harms, H. Fenton, N. E. Mandrak, and P. K. Molnár. 2023. Revealing large-scale parasite ranges: An integrated spatiotemporal database and multisource analysis of the winter tick. *Ecosphere* 14:43–76.
- DeCesare, N. J., T. D. Smucker, R. A. Garrott, and J. A. Gude. 2012. Moose status and management in Montana. *Alces* 50:35–51.
- Drew, M. 1984. Reproduction and transmission of the winter tick, *Dermacentor albipictus* (Packard) in central Alberta. M.Sc. Thesis, University of Alberta, Edmonton.
- Drew, M., and W. Samuel. 1985a. Factors affecting transmission of larval winter ticks, *Dermacentor albipictus* (Packard), to moose, *Alces alces* L., In Alberta, Canada. *Journal of Wildlife Diseases* 21:274–282.
- Drew, M., and W. Samuel. 1986. Reproduction of the winter tick, *Dermacentor albipictus*, under field conditions in Alberta, Canada. *Canadian Journal of Zoology* 64:714–721.
- Drew, M., and W. M. Samuel. 1985b. An evaluation of burning for control of winter ticks, *Dermacentor albipictus*, in central Alberta. *Journal of Wildlife Diseases* 21:313–315.
- Ellingwood, Daniel D, Peter J Pekins, Henry Jones, Anthony R Musante, D D Ellingwood, P J Pekins, H Jones, and A R Musante. 2020. Evaluating moose *Alces alces* population

- response to infestation level of winter ticks *Dermacentor albipictus*. *Wildlife Biology* 2020:1–7.
- Forrester, T. D., D. S. Casady, and H. U. Wittmer. 2015. Home sweet home: fitness consequences of site familiarity in female black-tailed deer. *Behavioral Ecology and Sociobiology* 69:603–612.
- Fullman, T. J., B. T. Person, A. K. Prichard, and L. S. Parrett. 2021. Variation in winter site fidelity within and among individuals influences movement behavior in a partially migratory ungulate. *PLOS ONE* 16.
- Garfelt-Paulsen, I. M., E. M. Soininen, V. Ravolainen, L. E. Loe, B. B. Hansen, R. J. Irvine, A. Stien, E. Ropstad, V. Veiberg, E. Fuglei, and Å. Ø. Pedersen. 2021. Don't go chasing the ghosts of the past: habitat selection and site fidelity during calving in an Arctic ungulate. *Wildlife Biology* 2021:1–13.
- Glines, M. V., and W. M. Samuel. 1989. Effect of *Dermacentor albipictus* (Acari:Ixodidae) on blood composition, weight gain and hair coat of moose, *Alces alces*. *Experimental & Applied Acarology* 6:197–213.
- Healy, C., P. J. Pekins, S. Atallah, and R. G. Congalton. 2020. Using agent-based models to inform the dynamics of winter tick parasitism of moose. *Ecological Complexity* 41:1–14.
- Healy, C., P. J. Pekins, L. Kantar, R. G. Congalton, and S. Atallah. 2018. Selective habitat use by moose during critical periods in the winter tick life cycle. *Alces* 54:85–100.
- Henningsen, J. C., A. L. Williams, C. M. Tate, S. A. Kilpatrick, and W. D. Walter. 2012. Distribution and prevalence of *Elaeophora scheinder* in moose in Wyoming. *Alces* 48:35–44.
- Holmes, C. J., C. J. Dobrotka, D. W. Farrow, A. J. Rosendale, J. B. Benoit, P. J. Pekins, and J. A. Yoder. 2018. Low and high thermal tolerance characteristics for unfed larvae of the winter tick *Dermacentor albipictus* (Acari: Ixodidae) with special reference to moose. *Ticks and Tick-borne Diseases* 9:25–30.
- Jin, S., C. Homer, L. Yang, P. Danielson, J. Dewitz, C. Li, Z. Zhu, G. Xian, and D. Howard. 2019. Overall methodology design for the United States national land cover database 2016 products. *Remote Sensing* 11.

- Jones, H., P. J. Pekins, L. E. Kantar, M. O'neil, and D. Ellingwood. 2017. Fecundity and Summer Calf Survival of Moose During 3 Successive Years of Winter Tick Epizootics. *Alces* 53:85–98.
- Jones, H., P. Pekins, L. Kantar, I. Sidor, D. Ellingwood, A. Lichtenwalner, and M. O'neal. 2019. Mortality assessment of moose (*Alces alces*) calves during successive years of winter tick (*Dermacentor albipictus*) epizootics in New Hampshire and Maine (USA). *Canadian Journal of Zoology* 97:22–30.
- Kauffman, M. J., E. O. Aikens, S. Esmaeili, P. Kaczensky, A. Middleton, K. L. Monteith, T. A. Morrison, T. Mueller, H. Sawyer, and J. R. Goheen. 2021. Causes, consequences, and conservation of ungulate migration. *Annual Review of Ecology, Evolution, and Systematics* 52:453–478.
- Laforge, M. P., M. Bonar, and E. Vander Wal. 2020. Tracking snowmelt to jump the green wave: phenological drivers of migration in a northern ungulate. *Ecology* 102.
- Lankester, M., and W. Samuel. 2007. Pests, parasites, and disease. Pages 479–517 *in*. *Ecology and Management of the North American Moose*. Second edition. The University Press of Colorado, Boulder, CO.
- MacHtinger, E. T., H. R. Springer, J. E. Brown, and P. U. Olafson. 2021. Sudden mortality in captive white-tailed deer with atypical infestation of winter tick. *Journal of Medical Entomology* 58:1962–1965.
- Mech, L. D., and J. Fieberg. 2014. Re-evaluating the northeastern Minnesota moose decline and the role of wolves. *The Journal of Wildlife Management* 78:1143–1150.
- Merkle, J. A., B. Abrahms, J. B. Armstrong, H. Sawyer, D. P. Costa, and A. D. Chalfoun. 2022. Site fidelity as a maladaptive behavior in the Anthropocene. *Frontiers in Ecology and the Environment* 20:187–194.
- Mooring, M. S., and W. M. Samuel. 1998. The biological basis of grooming in moose: programmed versus stimulus-driven grooming. *Animal Behaviour* 56:1561–1570.
- Musante, A., P. J. Pekins, and D. L. Scarpitti. 2007. Metabolic impacts of winter tick infestations on calf moose. *Alces* 43:101–110.
- Musante, A., P. Pekins, and D. Scarpitti. 2010. Characteristics and dynamics of a regional moose *Alces alces* population in the northeastern United States. *Wildlife Biology* 16:185–204.

- Nadeau, M. S., N. J. Decesare, D. G. Brimeyer, E. J. Bergman, R. B. Harris, K. R. Hersey, K. K. Huebner, P. E. Matthews, and T. P. Thomas. 2017. Status and trends of moose populations and hunting opportunity in the western United States. *Alces* 53:99–112.
- Nagelkerke, N. J. D. 1991. A note on general definition of the coefficient of determination. *Biometrika* 78:691.
- Nagy, D. W. 2004. *Parelaphostrongylus tenuis* and other parasitic diseases of the ruminant nervous system. *Veterinary Clinics: Food Animal Practice* 20:393–412.
- NCDC. 2020. Climate data online: dataset directory. 2020.
- Pekins, P. J. 2020. Metabolic and population effects of winter tick infestations on moose: unique evolutionary circumstances? *Frontiers in Ecology and Evolution* 8:1–13.
- Renecker, L. A., and R. J. Hudson. 1989. Ecological metabolism of moose in aspen-dominated boreal forests, central Alberta. *Canadian Journal of Zoology* 67:1923–1928.
- Ruprecht, J. S., K. R. Hersey, K. Hafen, K. L. Monteith, N. J. Decesare, M. J. Kauffman, and D. R. Macnulty. 2016. Reproduction in moose at their southern range limit. *Journal of Mammalogy* 97:1355–1365.
- Samuel, W. 2004. *White as a Ghost: Winter Ticks & Moose*. Volume 1. Federation of Alberta Naturalists, Edmonton, Alberta, Canada.
- Samuel, W. M., and D. A. Welch. 1991. Winter ticks on moose and other ungulates: factors influencing their population size. *Alces* 27:168–182.
- Sikes, R. S., and the A. C. and U. C. of the A. S. of Mammalogists. 2016. 2016 Guidelines of the American Society of Mammalogists for the use of wild mammals in research and education. *Journal of Mammalogy* 97:663–688.
- Sine, M., K. Morris, and D. Knupp. 2009. Assessment of a line transect field method to determine winter tick abundance on moose. *Alces* 45:143–146.
- Sullivan, C. F., B. L. Parker, A. Davari, M. R. Lee, J. S. Kim, and M. Skinner. 2020. Evaluation of spray applications of *Metarhizium anisopliae*, *Metarhizium brunneum* and *Beauveria bassiana* against larval winter ticks, *Dermacentor albipictus*. *Experimental & Applied Acarology* 82:559–570.
- Teitelbaum, C. S., S. Huang, R. J. Hall, and S. Altizer. 2018. Migratory behaviour predicts greater parasite diversity in ungulates. *Proceedings of the Royal Society B: Biological Sciences* 285.

- Turner, M. G. 1989. Landscape ecology: the effect of pattern on process. *Annual review of ecology and systematics*. Vol. 20 171–197.
- Wattles, D. W., and S. DeStefano. 2011. Status and management of moose in the northeastern United States. *Alces* 47:53–68.
- Welch, D. A., W. M. Samuel, and C. J. Wilke. 1990. *Dermacentor albipictus* (Acari, Ixodidae) on Captive Reindeer and Free-ranging Woodland Caribou. *Alces* 26:410–411.
- Welch, D. A., W. M. Samuel, and C. J. Wilke. 2011. Suitability of moose, elk, mule deer, and white-tailed deer as hosts for winter ticks (*Dermacentor albipictus*). *Canadian Journal of Zoology* 69:2300–2305.
- Wiseman, P. A., M. D. Carling, and J. A. Byers. 2006. Frequency and correlates of birth-site fidelity in pronghorns (*Antilocapra americana*). *Journal of Mammalogy* 87:312–317.

Tables

Table 2.1. Descriptions of covariates used to model spring resource selection by moose in Idaho, USA, 2020-2022. Data from both sources (National Land Cover Database, NLCD, and a digital elevation model, DEM) were at a 30 m resolution.

<i>Source</i>	
Covariate	Description
<i>NLCD</i>	
Evergreen Forest	Areas dominated by trees generally >5 m tall, and >20% of total vegetation cover. More than 75% of the tree species maintain their leaves all year. Canopy is never without green foliage.
Deciduous Forest	Areas dominated by trees generally >5 m tall, and >20% of total vegetation cover. More than 75% of the tree species shed foliage simultaneously in response to seasonal change.
Mixed Forest	Areas dominated by trees generally >5 m tall, and >20% of total vegetation cover. Neither deciduous nor evergreen species are >75% of total tree cover.
Herbaceous	Areas dominated by graminoid or herbaceous vegetation, generally >80% of total vegetation. These areas are not subject to intensive management such as tilling but can be utilized for grazing.
Shrub	Areas dominated by shrubs <5 m tall with shrub canopy typically >20% of total vegetation. This class includes true shrubs, young trees in an early successional stage or trees stunted from environmental conditions.
<i>DEM</i>	
Slope	Percent slope of topography
Aspect cosine	Cosine of aspect (North-South)
Aspect sine	Sine of aspect (East-West)
Topographic position	Values range from negative (valleys) to 0 (side slope) to positive (ridgelines).
Elevation	Elevation above sea level (m)

Table 2.2. Numbers and proportions of GPS locations of adult female moose within each National Land Cover Database (NLCD) cover type by study region, in Idaho, USA, during 15 March – 15 May of 2020-2022.

Region	Locations	Proportion of locations in each cover type				
		Evergreen Forest	Shrub	Herbaceous	Mixed Forest	Deciduous Forest
Selkirk	834	0.70	0.23	0.03	0.01*	<0.01*
Clearwater	1610	0.63	0.27	0.03	0.04	0.01*
Lost River	193	0.24	0.59	0.02*	0*	0*
Bannock-A	226	0.06	0.76	0.09	0.04	0.04
Bannock-B	1150	0.32	0.48	0.01*	0.01*	0.15
Island Park	213	0.30	0.49	0.01*	<0.01*	0.06

*Cover types containing <3% of locations within each region were not used in modeling.

Table 2.3. Top models of spring resource selection by adult female moose at the broad scale for each of six regions in Idaho, USA. Values are reported for number of model parameters (k), model weight (ω_i), and delta Akaike's Information Criterion (ΔAIC).

<i>Region</i>	Model	k	ω_i	ΔAIC
<i>Selkirk</i>	Evergreen Forest + Shrub + Herbaceous + Aspect Sine + Aspect Cosine + Elevation + Elevation ² + Slope + Slope ²	9	1	0
<i>Clearwater</i>	Evergreen Forest + Shrub + Herbaceous + Mixed Forest+ Aspect Sine+ Aspect Cosine + Elevation+ Elevation ² + Slope+ Slope ²	10	0.82	0
	Evergreen Forest + Shrub + Herbaceous + Mixed Forest+ Aspect Sine+ Aspect Cosine + Elevation+ Elevation ²	8	0.18	2.97
<i>Lost River</i>	Evergreen Forest + Shrub + Aspect Sine+ Aspect Cosine+ Elevation+ Elevation ² + Slope+ Slope ²	8	1	0
<i>Bannock-A</i>	Evergreen Forest + Shrub + Herbaceous + Mixed Forest+ Deciduous Forest + Aspect Sine + Aspect Cosine + Elevation + Elevation ² + Slope + Slope ²	11	1	0
<i>Bannock-B</i>	Evergreen Forest + Shrub + Deciduous Forest + Aspect Sine+ Aspect Cosine + Elevation + Elevation ² + Slope + Slope ²	9	1	0
<i>Island Park</i>	Evergreen Forest + Shrub + Deciduous Forest + Aspect Sine+ Aspect Cosine + Elevation + Elevation ²	7	0.86	0
	Evergreen Forest + Shrub + Deciduous Forest + Aspect Sine+ Aspect Cosine + Elevation + Elevation ² + Slope + Slope ²	9	0.13	3.72

Table 2.4. Top models of spring resource selection by adult female moose at the local scale for each of six regions in Idaho, USA. Values are reported for number of model parameters (k), model weight (ω_i), and delta Akaike's Information Criterion (ΔAIC).

<i>Region</i>			
Model	k	ω_i	ΔAIC
<i>Selkirk</i>			
NLCD type + Aspect Sine + Aspect Cosine + Slope+ Slope ²	6	0.68	0
NLCD type + Aspect Sine + Aspect Cosine + TPI+ TPI ² + Slope+ Slope ²	8	0.32	1.51
<i>Clearwater</i>			
NLCD type + Aspect Sine + Aspect Cosine + TPI+ TPI ² + Slope+ Slope ²	8	0.98	0
<i>Lost River</i>			
NLCD type + Aspect Sine + Aspect Cosine + TPI+ TPI ² + Slope+ Slope ²	8	1	0
<i>Bannock-A</i>			
NLCD type + Aspect Sine + Aspect Cosine + TPI+ TPI ² + Slope+ Slope ²	8	0.92	0
<i>Bannock-B</i>			
NLCD type + Aspect Sine + Aspect Cosine + TPI+ TPI ² + Slope+ Slope ²	8	0.93	0
<i>Island Park</i>			
NLCD type + Aspect Sine + Aspect Cosine + TPI+ TPI ² + Slope+ Slope ²	8	0.86	0
NLCD type + Aspect Sine + Aspect Cosine + Slope+ Slope ²	6	0.14	3.69

Table 2.5. Models predicting relative burden of winter ticks as a function of use of the tick risk landscape for moose in in 6 study regions across Idaho, USA, 2020-2022. Values are reported for maximized log-likelihood ($\log(L)$), Akaike's Information Criterion (AIC_c), Nagelkerke's pseudo R^2 , delta AIC_c (ΔAIC_c), and AIC weight (ω_i).

Model	$\log(L)$	AIC	R^2	ΔAIC	ω_i
~ tick risk value + study region	-78.95	173.91	0.26	--	0.70
~ study region	-81.27	176.54	0.20	2.63	0.19
~ tick risk value	-86.47	178.94	0.08	5.03	0.06
~ tick risk value + (1 study region)	-85.77	179.54	0.10	5.63	0.04
~ 1	-89.48	182.96	0.00	9.05	0.01

Table 2.6. Coefficient estimates and 90% confidence intervals from the top-ranked model for predicting relative tick burden on moose as a function of use of the tick risk landscape in Idaho, USA, 2020-2023. Beta estimates (β) for tick count bins (low, medium, high) can be interpreted as the log odds of moving from one bin to the next based on a one unit increase in tick risk value.

Coefficient	Estimate (β)	90% CI
Low medium	0.94	0.39-2.27
Medium high	6.49	2.48-16.95
Tick risk value	1.03	1.01-1.06
Clearwater region	1.94	0.72-5.26
Lost River region	0.13	0.02-1.05
Bannock-A region	0.09	0.01-0.73
Bannock-B region	1.67	0.39-7.03
Island Park region	1.98	0.47-8.41

Figures

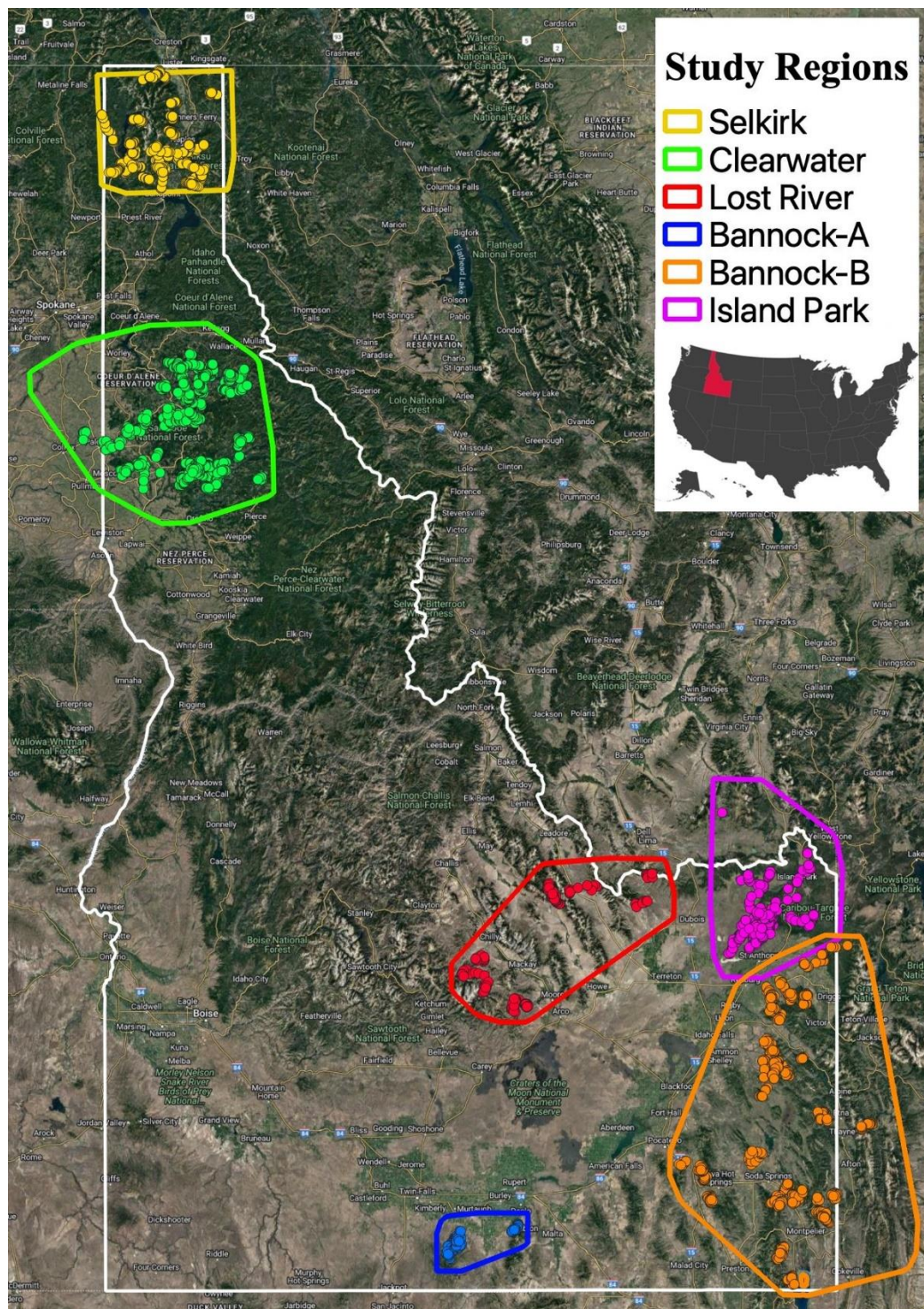


Figure 2.1. Study regions (polygons) and GPS locations (circles) used to model spring habitat selection by adult female moose within each region in Idaho, USA, 2020-2022.

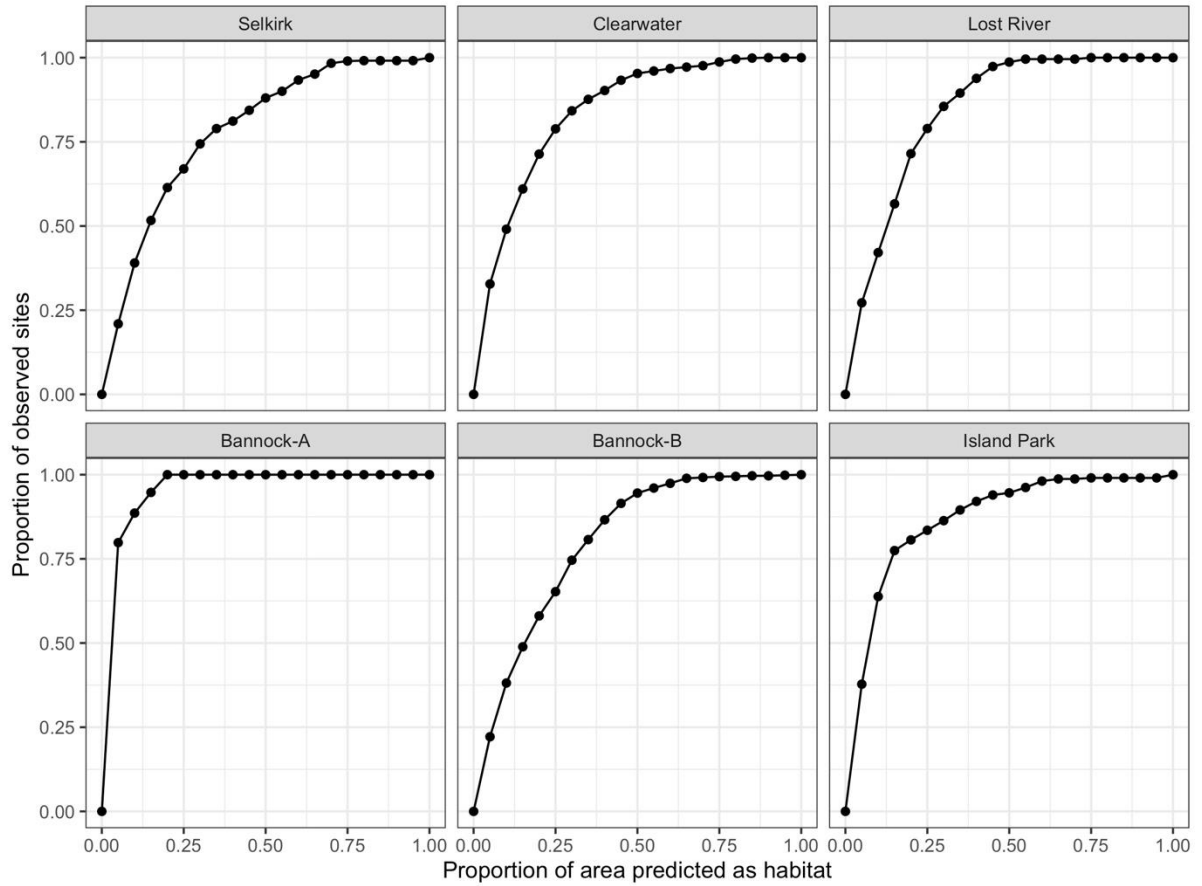


Figure 2.2. Specificity vs. sensitivity plots of the final predictions of spring moose habitat (AUC=; 0.70-0.92) by study region in Idaho, USA, 2020-2022.

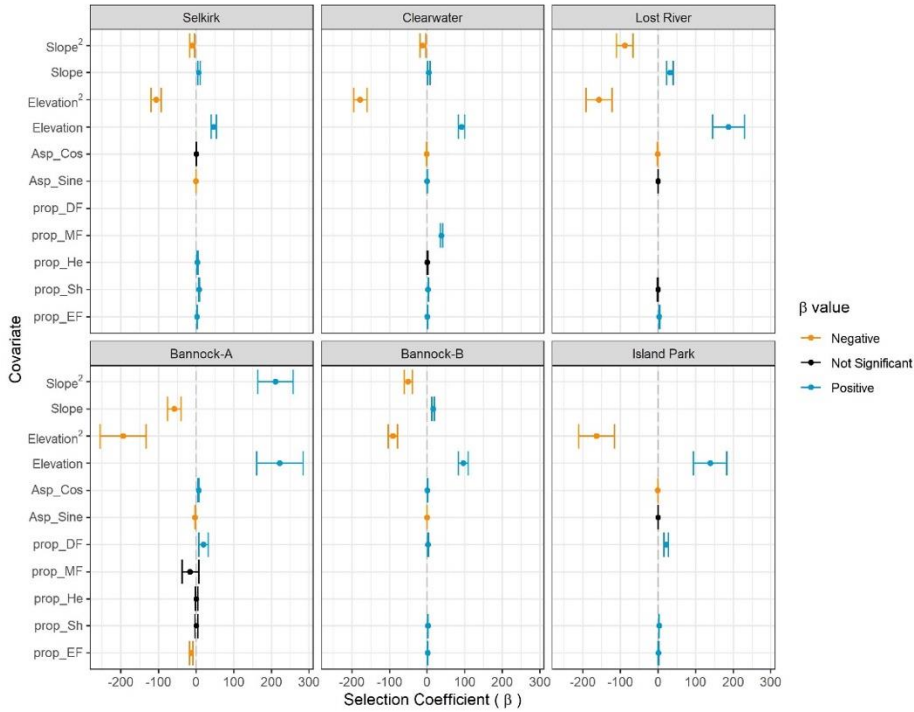


Figure 2.3. Parameter estimates (\pm 95% CI) from the top broad-scale models of spring resource selection by adult female moose in six regions of Idaho, USA, 2020-2022.

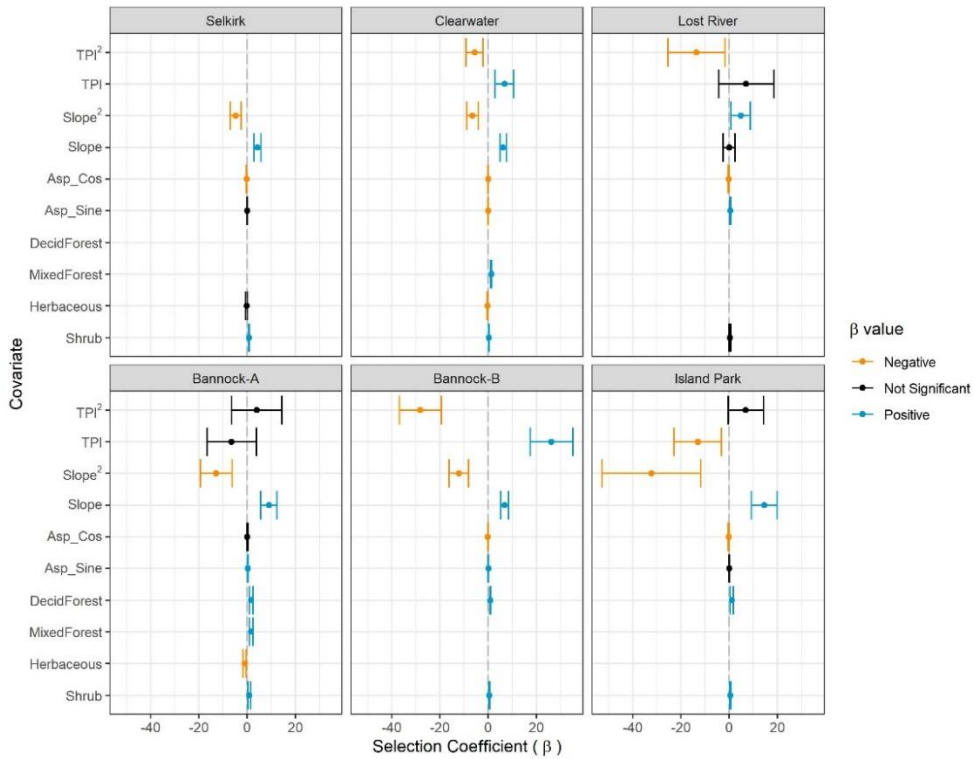


Figure 2.4. Parameter estimates (\pm 95% CI) from the top local-scale models of spring resource selection by adult female moose in six regions of Idaho, USA, 2020-2022.

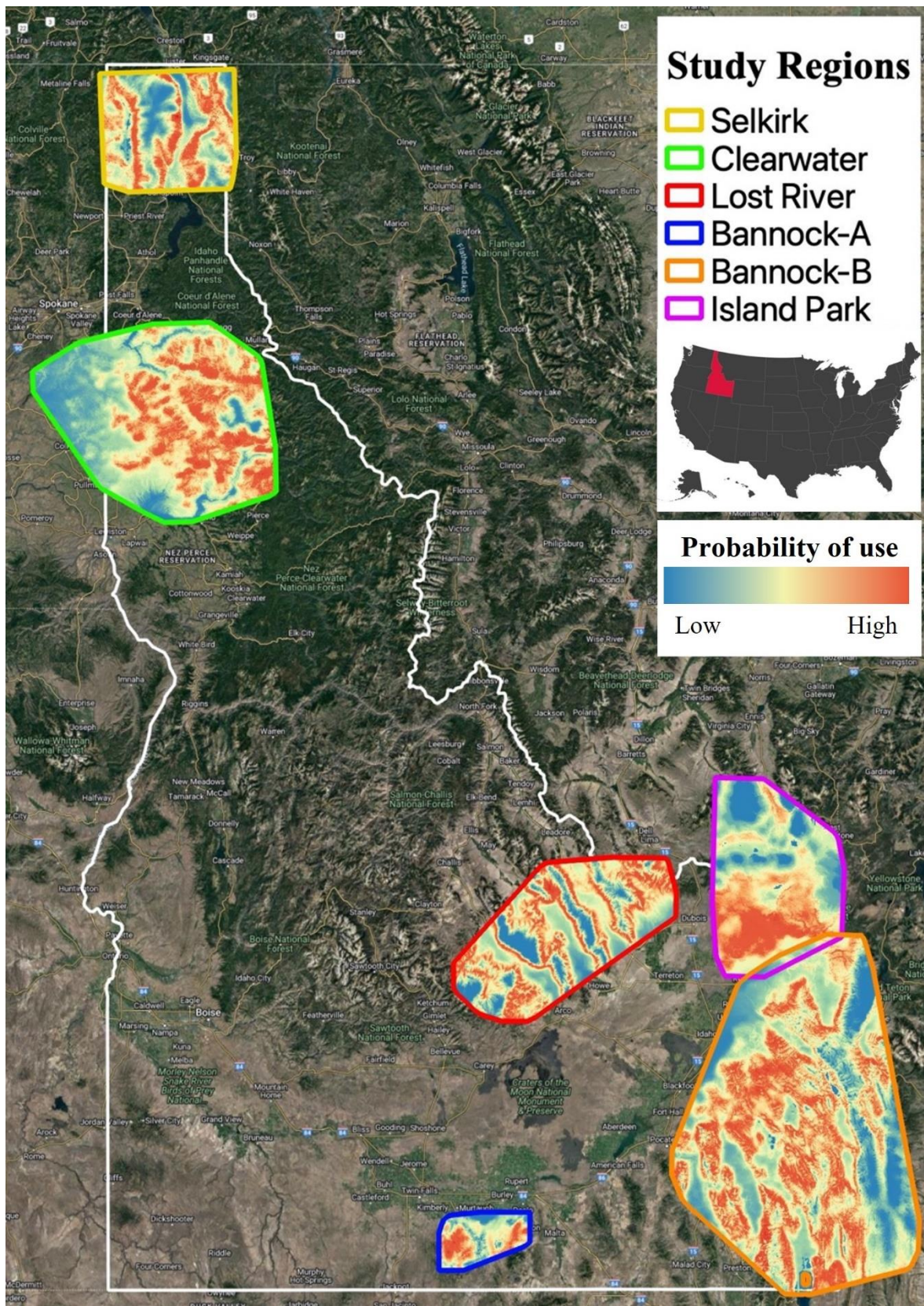


Figure 2.5. Tick risk landscapes estimated as the relative probability of use of habitat by adult female moose during the spring winter tick drop-off period in six study regions in Idaho, USA, 2020-2022.

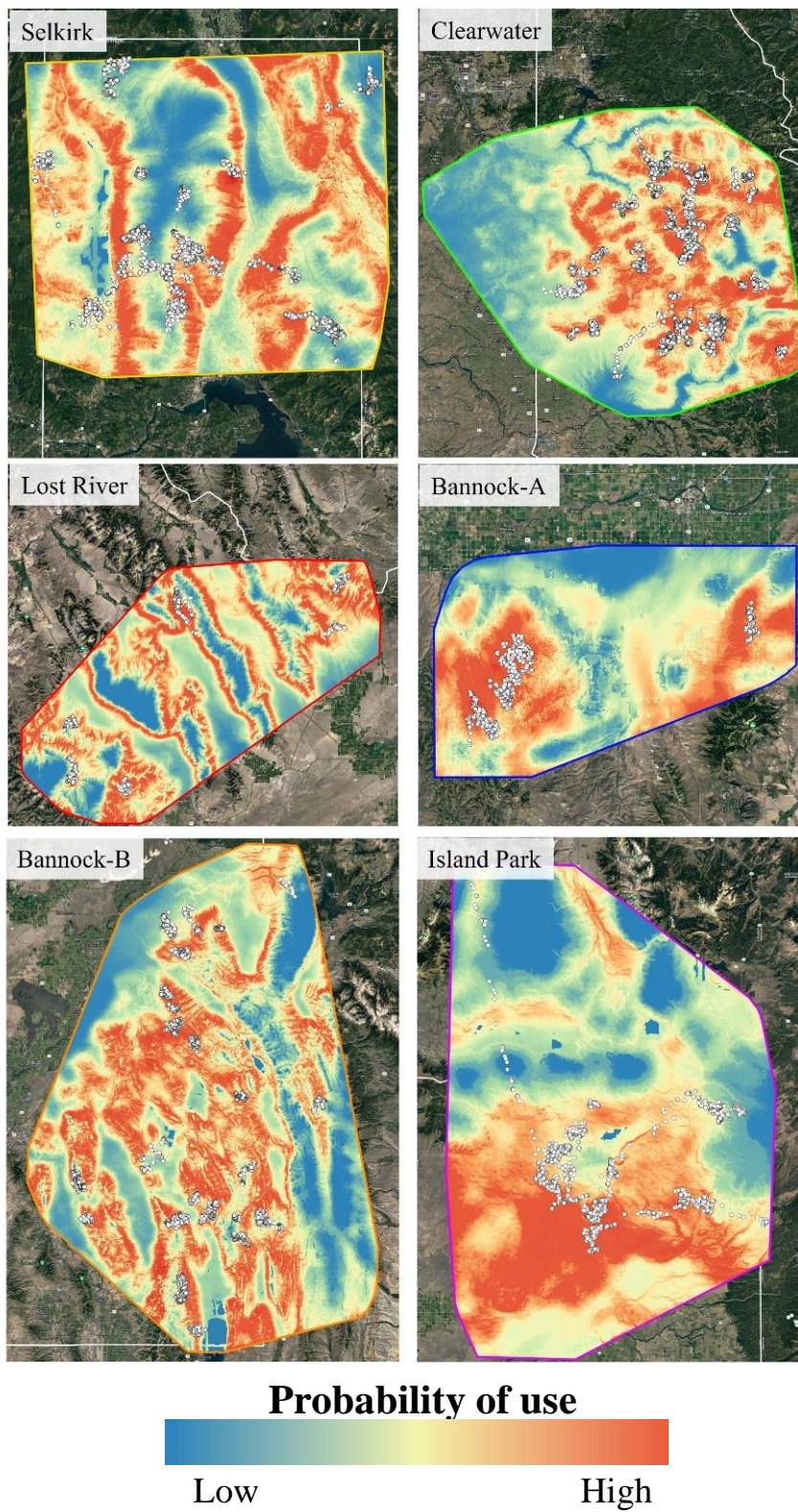


Figure 2.6. Regional tick risk landscapes estimated as the relative relative probability of selection of habitat by adult female moose during the spring winter tick drop-off period in six study regions in Idaho, USA, 2020-2022. Locations of GPS collared females during the fall tick pick-up period are represented by circles.

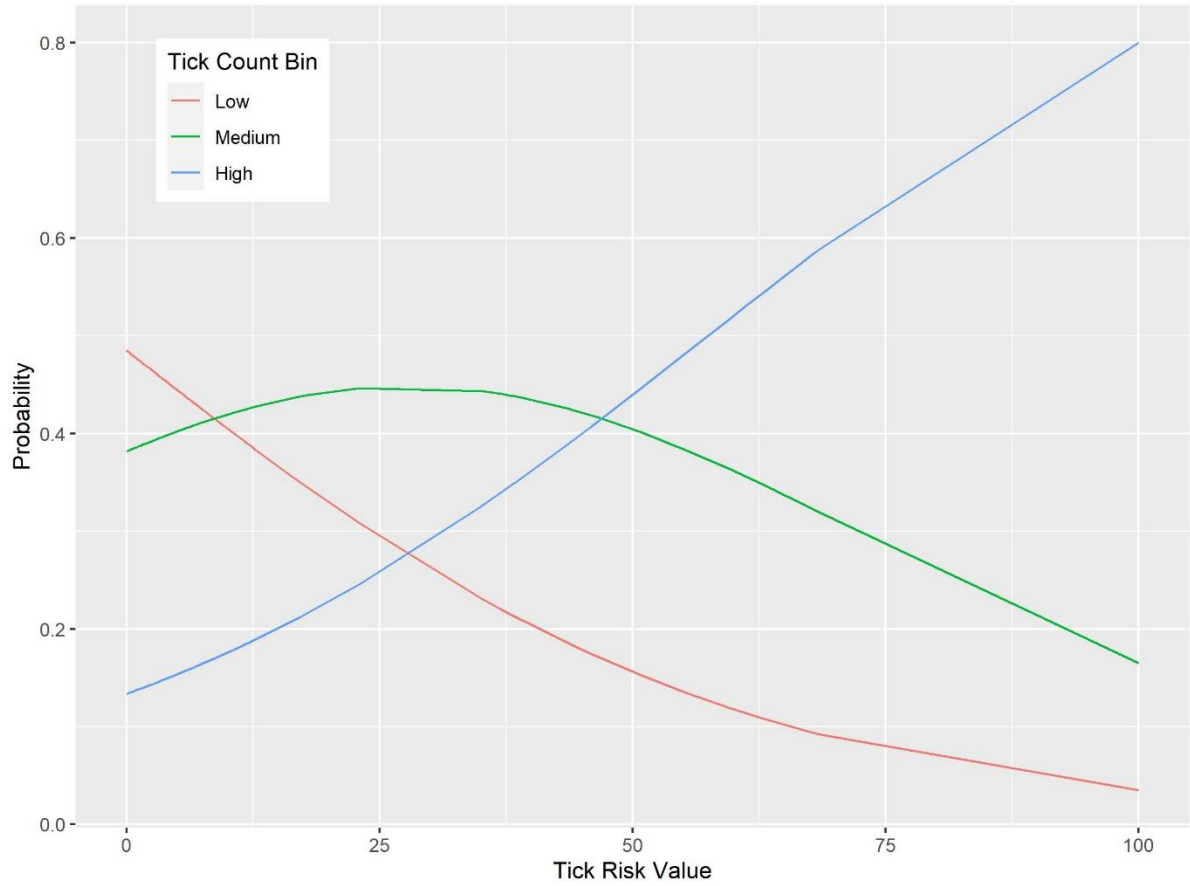


Figure 2.7. Predictions from the top model for predicting relative winter tick burden on moose as a function of use of the tick risk landscape across 6 study regions in Idaho, USA, 2020-2022. Moose were more likely to acquire a high tick load with increased exposure to the tick risk landscape.

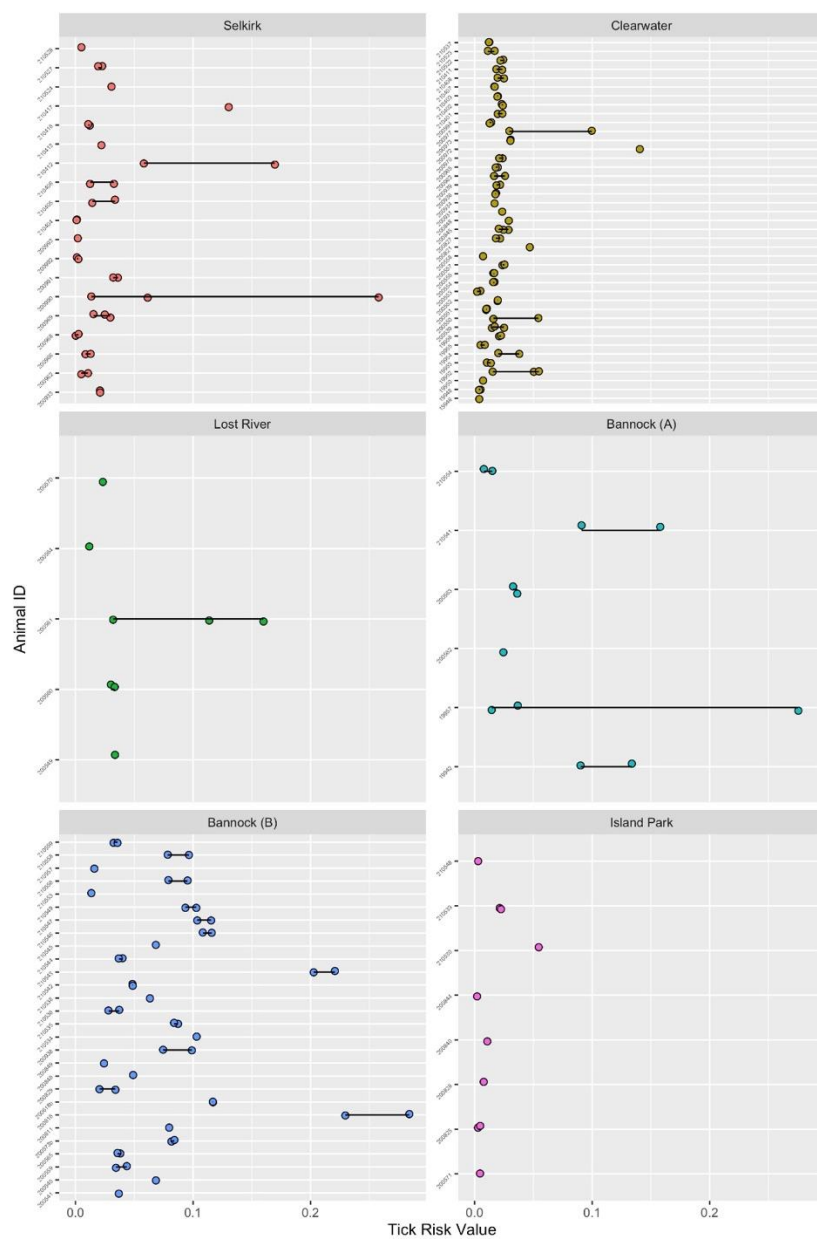


Figure 2.8. Annual estimated exposure of moose to the tick risk landscape in Idaho, USA, 2020-2022. Dots represent individual tick risk values for 1-3 years for which data were available, with black lines connecting individuals across years. For individuals with 2-3 years of fall location data, the coefficient of variation ($n = 50$, mean = 0.05) did not differ significantly from zero (p -value = 0.03), indicating comparable exposure to the winter tick risk landscape across years.